Investigating Protein-Membrane Interactions Mediated by Factor X that Regulate the Blood Clotting Cascade

by

Divyani Paul

A dissertation submitted in partial fulfillment
of the requirements for the degree of
Doctor of Philosophy
(Biological Chemistry)
in the University of Michigan
2022

Doctoral Committee:

Professor James H. Morrissey, Chair
Professor Ryan C. Bailey
Assistant Professor Ryan D. Baldridge
Professor Ruma Banerjee
Professor Phyllis I. Hanson

Divyani Paul

divyani@umich.edu

ORCID iD: 0000-0002-4544-1825

Dedication

This dissertation is dedicated to my parents for their loving support, encouragement, and guidance throughout my life. I would also like to dedicate this dissertation to all my teachers who have taught me important lessons that have shaped my career.

Acknowledgements

Support from my mentors, colleagues, friends, and family has helped me to successfully conduct research and share my work with the scientific community. I would like to thank my advisor, Dr. Jim Morrissey, for introducing me to the interesting world of protein-membrane interactions in blood clotting that I pursued to study during my doctoral research. Besides imbibing scientific knowledge from Jim, I have also learned important soft skills such as paying attention to details, which shall help me to do well in my future as well. Most importantly, Jim always gave me the scientific freedom of conducting research and has supported me in achieving my career goals. I would also like to thank former lab member Dr. Yan Wang for teaching me several techniques which I continued utilizing during my doctoral research.

Another pillar of support in this journey was provided to me by the members of my thesis committee. Every feedback from the committee encouraged me to dive further into the literature to understand the field better. Early on from my prelim committee to the completion of my thesis, Dr. Ruma Banerjee helped me to become a cognizant scientist. Dr. Ryan Baldridge was always welcoming and provided me with amazing ideas to pursue. Dr. Ryan Bailey strengthened my research by giving me the opportunity to collaborate with his lab and utilize their amazing technique of high throughput micro-ring resonators to address important questions in my research. Dr. Phyllis Hanson provided tremendous support and helped me during challenging times. This research would not have been possible without the help of my collaborators who also became my good friends during this journey. I would like to thank Dr. Sara Medfisch, Melanie Muller, Muyun Lihan and Dr. Ashley De Lio for their valuable contributions towards my thesis chapters. I'm also thankful to Dr. Anne Vojtek and Beth Goodwin who have always listened to my difficulties and helped me overcome them as a graduate student.

I'm thankful to my father who has inspired me since I was a little girl to become a scientist like him. It has been a long journey and my parents always kept me grounded and focused to come this far. Lastly, I would like to thank my dear friends who have celebrated my successes, eased my sorrows, and gave me wonderful experiences.

Table of Contents

List of Tables

List of Figures

Abstract

Vascular trauma triggers the blood clotting cascade to maintain hemostasis by sequentially converting several zymogens to active enzymes via limited proteolysis. Coagulation factor X (FX) is activated by the extrinsic and intrinsic pathway to initiate and propagate the clotting cascade respectively. Further, activated FX (FXa) also participates in downstream reactions in the common pathway that leads to the formation of a blood clot, thereby, positioning FX centrally in the clotting cascade. Anionic membrane surfaces accelerate the activation of FX by thousands of times, underscoring the regulatory function of protein-membrane interactions in the clotting cascade. The N-terminal, γ-carboxyglutamate rich domain (Gla-domain) enables FX to reversibly bind phosphatidylserine (PS), in a calcium dependent manner. Previous studies showed that removing the Gla-domain diminished the rates of FX activation by the initiation complex even in solution, which indicates the participation of Gla-domain in protein-protein interactions as well. This demonstrates that FX Gla-domain plays a crucial role in the blood clotting cascade. However, these interactions of FX Gla-domain are poorly characterized at the molecular level. Therefore, here we investigated these interactions from the perspectives of the membrane phospholipids and clotting proteins that directly interact with FX Gla-domain.

Quantitative binding studies were utilized to identify the stoichiometry of membrane lipids binding to FX Gla-domain in physiologically comparable membrane surfaces. Here for the first time, we present the evidence for a unique PS binding site in the FX Gla-domain. Next, we employed mutagenesis studies of FX Gla-domain residues to identify their impact on the rates of FX activation by the initiation complex of the clotting cascade. Along with additional membrane binding studies we identified the critical amino acid residues in the FX Gla-domain that participate in either protein-protein or membrane-protein interactions in the extrinsic pathway.

A potent external activator of FX from Russell's Viper Venom (also known as RVV-X) causes thrombotic complications in snake-bite victims, ultimately resulting in their death or disability. However, due to the high potency of RVV-X it has also been used to treat minor injuries and as a diagnostic tool in research. Biochemical studies showed that in absence of the Gla-domain,

RVV-X poorly activates FX. Therefore, we extended our study to identify the residues mediating molecular interactions between FX Gla-domain and RVV-X. FX Gla-domain residues predicted to interact with RVV-X by *in silico* structural alignment studies were mutated to test their influence on the rates of FX activation by RVV-X. FX activated by RVV-X was utilized to investigate the effects of the mutated residues on the thrombin generation. Thus, we identified the key residues in FX Gla-domain essential for mediating the molecular interactions between FX and RVV-X. Surprisingly, we observed that the FX Gla-domain residues crucial to the extrinsic pathway, had a minimal impact on thrombin generation in the common pathway.

Since several clotting reactions occur on membrane surfaces, we diversified our study beyond the molecular interactions of FX Gla-domain. We found that an anticoagulant protein, lactadherin, exhibited membrane binding in a calcium independent manner. These findings will aid in the development of therapeutic efforts against pathological conditions such as thrombosis and bleeding disorders in FX deficient patients.

Chapter 1 Role of Factor X in the Blood Clotting Cascade

1.1 Introduction

Blood coagulation factor X (FX) is an important component of the coagulation cascade. It is a 59kDa trypsin like serine protease, which circulates as an inactive zymogen in the plasma at a concentration of 10µg/ml with a half-life of 20-40h[1]. The coagulation cascade functions via the extrinsic and intrinsic pathway that converges at the crucial step of FX activation from its zymogenic state. In the extrinsic pathway, FX is activated by a two-subunit enzyme composed of tissue factor (TF) and factor VIIa (FVIIa). TF is an integral membrane protein expressed externally on the epithelial tissues surrounding blood vessels. Upon vascular damage, the "extrinsic" TF comes in contact with plasma factor VII (FVII) in the lumen of the blood vessel to form the "extrinsic tenase" complex and initiates the clotting cascade. Interactions between FVII and TF results in the generation of active FVII (FVIIa) through limited proteolysis. FVIIa itself is a poor enzyme but pairing up with TF increases its ability to activate FX by 20-100 fold.[2, 3] In the intrinsic pathway, activated factor

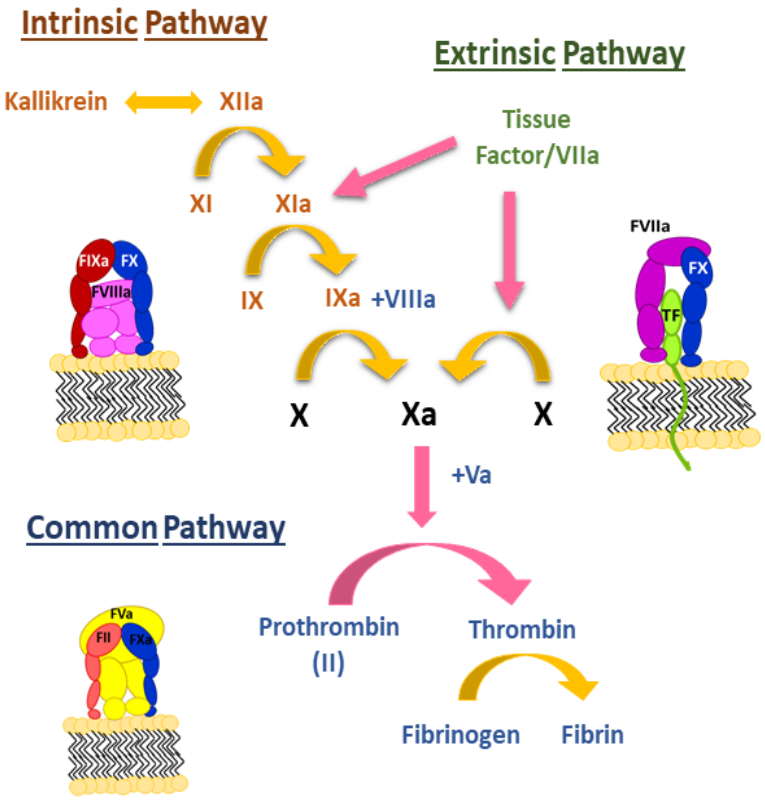

Figure 1.1 **Extrinsic, Intrinsic and Common Pathway of the clotting cascade**. Clotting reactions occurring on the membrane surfaces show are represented with pink arrows.

IX (FIXa) forms a complex with activated factor VIII (FVIIIa), also known as the "intrinsic tenase" complex to generate activated FX (FXa). Eventually, FXa is responsible for generating the "thrombin burst" in the common pathway of the cascade for successful clot formation. FXa along with its cofactor activated factor V (FVa) forms the "prothrombinase" complex which converts prothrombin to thrombin. All three complexes, assemble on anionic membrane surfaces in presence of calcium ions (Ca^{2+}) to enhance the localized catalytic rate of substrate activation.[4] Stereospecific interactions between the γ-carboxyglutamate-rich domain (Gla domain) of FX and phosphatidylserine (PS) headgroup present on the membrane surface is a prerequisite for FX function.[5] FX also interacts with anticoagulation proteins Tissue Factor Pathway Inhibitor (TFPI) and antithrombin.[6, 7] Being placed at the node of three pathways in the clotting cascade Figure 1.1, makes FX a suitable drug target for thrombotic diseases. In this review, we discuss the structural requirements of FX for interacting effectively with a wide range of clotting factors and the membrane.

1.1 FX protein structure

Human coagulation FX is a 59 kDa protein encoded by a 22kb gene located on the long arm of chromosome 13q34.[8] It is synthesized as a single-chain precursor molecule in liver. FX precursor protein contains a signal peptide and a propeptide that are removed during post-translational processing within the cell. During or after secretion from the liver, the amino acid sequence, Arg-Lys-Arg (140-142) is cleaved to generate a light chain (amino acids 1-139) and a heavy chain (amino acids 143-448), linked covalently by a disulfide bond. The light chain of a FX molecule starts with the (γ-carboxyglutamate-rich) domain also known as the Gla domain. The Gla residues are a result of post-translational modification of glutamate residues by the enzyme Vitamin K dependent γ-glutamyl carboxylase.[9] In the liver, the carboxylase recognizes the ~ 18 amino acid long propeptide of FX and converts 11 Glu residues to Gla residues. Gla domains commonly found in the

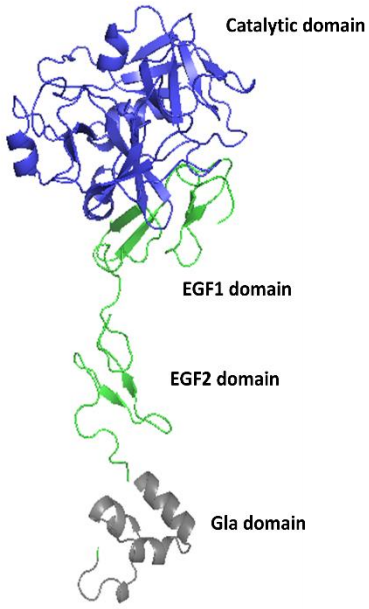

Figure 1.2 FX molecular model was designed by Melanie Muller at University of Illionis, Urbana Champaign. This model highlights the various domains of FX.

family of vitamin K-dependent blood clotting proteins, allow them to bind membranes in a calcium dependent manner, which is key to the complex formation in the clotting cascade. Aromatic amino acid residues 40-45 connect the Gla domain to two Epidermal Growth Factor like domains (EGF1 residues 46-84 and EGF2 85-128). Another post-translational modification of Asp 63 in the EGF1 domain to β-hydroxyaspartate acid, provides a weak calcium binding site that is critical for the correct conformation of the FX molecule.[10, 11] To summarize, the ability to bind membranes and interact with other protein partners in the clotting cascade by assuming the correct conformation is conferred by the light chain leaving the catalytic property to the heavy chain of the FX molecule. The heavy chain of FX molecule begins with the activation peptide (AP) domain (Ser 143-Arg194) which is succeeded by the serine protease (SP) domain (amino acids 195-448). Removal of AP by proteolytic cleavage of the peptide bond between Arg 194-Ile 195 releases the active enzyme FXa needed for thrombin formation. FXa is a trypsin like serine protease which harbors the catalytic triad of His236-Asp282-Ser379. It has been suggested, that upon activation of the zymogen FX, significant reorientation of the SP domain occurs, and the N-terminal Ile 16 is projected into the core of the SP domain.[12] The various FX domains are shown in Figure 1.2. Lastly, post translational modification of N-glycosylation in the AP is consequential in FX activation since the removal of the amino acid residues that serve as the glycosylation site drastically reduces FX activation by intrinsic and extrinsic tenase complex.[13]

1.2 Structure-function relationship of FX

1.2.1 Molecular interactions between FX/FXa and TF/FVIIa complex

Activation of FX by TF/FVIIa or "extrinsic tenase" complex, initiates the clotting cascade. FXa can also reciprocally activate TF/FVII for additional blood clotting reactions.[14, 15] Human TF is a ~46kDa transmembrane protein with no enzymatic activity. It consists of an N-terminal extracellular domain (amino acids 1-219), a transmembrane domain (amino acids 220-242) and a C-terminal cytoplasmic tail (amino acids 243-263).[16] Human FVIIa, is an ~50kDa protein, which includes N-terminal Gla domain, two EGF-like domains and a C-terminal SP domain. The poor enzyme activity of free FVIIa is enhanced drastically upon binding to TF and induces conformational changes in FVIIa via allosteric interactions to enhance the rate of FX activation by almost a million fold.[3, 17] The successful assembly of the ternary complex of TF/FVIIa/FX or

TF/FVII/FXa depends significantly on protein-protein interactions, which will be discussed in this section. While the structure of the ternary complex remains unsolved, the Scripps group (Ss/Se models) and the Chapel Hill group (CheA/CheB models) proposed a model for the ternary complex using molecular docking to identify possible contacts between TF/FVIIa and FX.[18, 19] *In silico* solvent equilibration of the ternary complex for 10ns showed the following important domain-domain interactions: 1) The Gla domain of FX interacts with both TF and the Gla domain of FVIIa, 2) The EGF1 domain of FX interacts with TF and the EGF2 and the SP domain of FX interacts with the SP domain of FVIIa.[20] Site directed mutagenesis studies and fluorescence probing of TF residues indicate amino acids from 157-167,200 and 201 interact with the Gla and EGF1 domain of FX.[21, 22] Residues Lys 165 and 166 in TF were identified to interact with FX in a membrane dependent manner.[23] In vitro, studies showed that mutating Lys 165 or Lys 166 to Ala reduced FX-WT activation rates (~80%) but the effect of TF exosite mutants were absent on the activation rates of Gla-domainless FX (GD-FX), which suggested interactions between the Gla domain of FX and TF near the membrane plays a role in FX activation by the extrinsic tenase complex.[24] Ala substitution mutants of TF, Arg200 and Lys201 were evaluated for their ability to activate wild-type FX (FX-WT), GD-FX and FX lacking both Gla and EGF1 (FX-E2) domain. The activation rates of FX-WT and GD-FX were impaired except FX-E2 suggesting the EGF1 domain interacts with TF at Arg 200 and Lys 201.[25] The Ss/Se models also provide corroborating evidence of FX residues Gla32, Asp 35 and Gla 39 forming salt bridges with Lys166,Arg200 and Lys201.[18] Several studies with FX chimeric molecules provide substantial evidence for interactions between various domains of FX with TF/FVIIa complex.[26-28,29,30] Replacing the Gla and EGF1 domain of FX with that of coagulation factor IX (IX) and protein C markedly reduced the affinity of FX towards the TF/FVIIa complex resulting in reduced FX activation rates.[26, 29] FX activation rates were reduced by 740-fold upon activation by Gla-domainless FVIIa (GD-FVIIa) in complex with TF and membranes as compared to WT-FVIIa indicating direct interactions between the Gla domains of FX and FVIIa.[30] The Che/CheB model proposes ionic interactions between Gla 14 residue of FX-Gla domain and Arg36 in the FVIIa Gla domain which was identified independently by mutagenesis studies.[19, 31] Interactions between the light chain of FX and its enzyme TF/FVIIa are primary recognition determinants for the ternary complex formation. The binding between FX and TF/FVIIa stabilizes the complex formation and allows correct positioning of SP domain of FX to be cleaved by FVIIa. Unlike other serine proteases FVIIa lacks the oxyanion hole.[32] In the

correct orientation the scissile peptide bond in FX occupies the active site in FVIIa which induces formation of the oxyanion hole for FX activation.[33] Kinetic studies of the FVIIa SP domain show that amino acid residues 285-305 are involved in recognition of FX and that Arg 290 is important for proteolytic cleavage of FX.[34]

1.2.2 Molecular interactions between FX/FXa and FIX/FVIIIa complex

The intrinsic pathway also leads to FX activation by activated clotting factor IX (FIXa) bound to its cofactor, activated factor VIII (FVIIIa). After initiation of the clotting cascade by extrinsic tenase complex, the intrinsic pathway is responsible for the propagation of the clotting cascade. Deficiency of FIX or FVIII results in hemophilia A or B which underlines the importance of the intrinsic pathway. Human FIXa, is a 44kDa two chain vitamin-K-dependent serine protease and activates FX while FVIII, is a single chain 300kDa protein comprising a heavy chain (A1-A2-B) and a light chain (A3-C1-C2) domain. By positive feedback, FXa converts FVIII to FVIIIa by proteolytic cleavage at the Arg336 site.[35] Consequently, FVIIIa enhances the rate of FX activation by FIXa by 200,000 fold.[36] FX is brought in close proximity to its activating enzyme FIXa by FVIIIa on membrane surfaces. Direct binding assays of FX to isolated domains of FVIIIa revealed that FX interacts with the A1 subunit of FVIIIa in presence of Ca^{2+}. Competitive binding studies of FX between the C-terminal of the A1 (residues 337-372) and the entire A1 domain showed that FX binds more tightly to the C-terminal suggesting that the FX binding site is present in the C-terminal of the A1 domain of FVIIIa.[37] This observation is further supported by crosslinking studies that confirmed the interaction between the SP domain of FX and the C-terminal of FVIIIa.[38] While FX interacts with FVIIIa at the A1 subunit, FIXa interacts at the A2 subunit resulting in the "intrinsic tenase" complex formation. In FIXa, the residues 102-106 in the third loop of EGF2 domain provides the binding site for FX. Replacing these residues in FIXa with that of FVII and FX resulted in decreased rates of FX activation.[39] In addition Ala substitution of EGF2 residues 102-106 had no effect on FIXa binding to FVIIIa but reduced the catalytic ability of FIXa towards FX, thus confirming their role in activation of FX.[40]

1.2.3 Molecular interactions between FXa and FVa and prothrombin

FXa generated by the extrinsic and the intrinsic pathway, interacts with factor Va (FVa) to cleave the zymogenic prothrombin to active thrombin in the common pathway. The rate of thrombin generation is enhanced by about 300,000-fold because of complex formation between FXa and FVa on membrane surfaces in presence of calcium, also known as the prothrombinase complex. Factor V (FV), is a 330kDa protein that circulates as a single chain protein in plasma with A1-A2-B-A3-C1-C2 domains. Removal of the B domain by thrombin leaves a two-chain protein known as FVa, comprising of the heavy chain (A1-A2 domains) and the light chain (A3-C1-C2 domains). Biochemical studies show a highly basic region exposed to the solvent in FXa involving residues Lys-276, Lys-351, Arg-306, Lys-414, Lys-420 and Arg-424 is a FVa binding site. Mutating these residues to Ala impaired their ability to bind FVa and in particular Arg-347 and Lys-351 greatly reduced the ability of thrombin generation by FXa and cofactor FVa.[41-43] Residues 493-506 and 311-325 in FVa constitutes the binding site for FXa.[44, 45] Crystal structure of the high-affinity and membrane independent FX-FV complex from the venom of the snake, *P textilis,* was adopted for building homology models of human prothrombinase complex which provides more structural insight into the complex.[46, 47] In agreement with the biochemical data, the homology model of human prothrombinase complex shows the basic residues in FXa, forms a network of salt bridges and hydrogen bonds to acidic residues 657-669 in the A2 region in FVa. Additionally, both EGF1 and EGF2 domains of FXa interacts with the A3 domain of FVa but FX-Gla domain does not make any contact in this model.[47] Prothrombin (PT) , a 72kDa protein docks on the macromolecular complex of FXa-FVa to become activated thrombin. PT contains N-terminal Gla domain, two kringle domains and a C-terminal trypsin like serine protease domain. FXa cleaves PT at Arg-320 to generate meizothrombin which is followed by another cleavage at Arg271 to generate mature α-thrombin. Mutating Lys-96 impaired the catalytic efficiency of FXa towards PT by 5-10 fold suggesting this residue to be in direct contact with PT.[48] Further, insight into the interactions between FX and PT is provided by an all atom human ternary complex which is built based on the available crystal structures of FX-FV complex of *P texilis.* The ternary complex model incorporates the two loops of PT containing residues Arg271 and Arg320 near the FXa active site. This model predicted that the sulphotyrosines in the A2 domain of FVa trap the SP domain of PT from solution and secures a position in the FXa active site for successful cleavage of PT to thrombin.[49]

1.3 Role of FX in the anticoagulation system

The tight regulation of hemostasis is dependent on the naturally occurring anticoagulants which inhibit the protease function of the clotting factors by directly inhibiting them or their cofactors. The anticoagulants prevent the formation of accidental or pathological thrombi to protect humans from life threatening diseases such as atrial thrombosis, venous thromboembolism (VTE) and pulmonary embolism (PE).[50] Tissue factor pathway inhibitor (TFPI) is the primary inhibitor of the ternary complex of TF-FVIIa-FXa, which is responsible for initiation of the clotting cascade. TFPI is a 34kDa single chain polypeptide synthesized by the vascular endothelium and circulates in the plasma at low concentration levels of ~2.5nM.[51] Alternative splicing of the TFPI gene gives rise to two major isoforms known as TFPIα and TFPIβ. TFPIα consists of a N-terminal acidic region followed by three specialized Kunitz domains (K1, K2 and K3) and a C-terminal basic region and the three Kunitz domains are joined by two linker regions (L1 and L2). Alternative RNA splicing results in the loss of the third Kunitz (K3) domain in TFPIβ. Since the inhibitory effect of TFPI is mediated by the binding event of K1 to the active site of FVIIa and K2 of FXa,[52] both the isoforms can impair the initiation of the clotting cascade. For a detailed understanding of the inhibitory mechanisms of the TFPI isoforms see the review by Wood et al.[53] The second Kunitz domain (K2) of TFPI inhibits FXa with a K_i of 1.5×10^{-10} M. With the help of NMR derived TFPI-K2 domain structures and computational modelling and MD simulation studies of TFPI-K2-FXa complex it was inferred that the interactions between the three surface loops of FXa (the 39-loop, the 60 loop and the 148-loop) and the TFPI-K2 domain contributes towards the high inhibitory effect of TFPI and most of the interactions outside the loop region were dominated by electrostatics. Further, the formation of the TFPI-K2-FXa complex required reorganization of the residue Tyr-99 in active site of FXa with the help of hydrophobic interactions between Trp-215 and Phe-174 residues in FXa and Ile-13, Leu-39 and Cys14—Cys38 in TFPI-K2 domain.[54] Additional modelling studies highlighted the basic nature of Arg-15 in the K2 domain of TFPI allows it to penetrate into the active site of FXa protease and Tyr-17, Arg-32 and Glu-46 confers specificity of the TFPI domain towards FXa.[55] Although the K2 domain is responsible for interacting specifically with FXa, it has been observed that the binding affinity of full length TFPI is 1000-fold higher as compared to the isolated K2 domain.[56] Mutating the C-terminus of the TFPI

reduces the rate of FXa inhibition by ~ 6-fold.[57] The inhibition of FXa by TFPI is a biphasic reaction that is observed as a slow-tight binding mechanism.[58] FXa and TFPI first form a loose binary complex which slowly isomerizes to a tight FXa-TFPI complex.[59] The ultimate goal of TFPI to inhibit the extrinsic tenase complex requires the interaction of the Gla domain with TFPI.[60] Since the Gla domain of FXa is highly acidic, it is thought to interact with the basic C-terminal region of TFPI and this interaction is enhanced in presence of phospholipids and Protein S .[61-63]

FXa is also inhibited by another serine protease inhibitor (serpin) known as Antithrombin (AT).[64] Free AT circulating in blood at a high concentration of 2.3μM is a relatively weak inhibitor of FXa. Upon allosteric activation of AT III by a pentasaccharide the rate of inhibition is accelerated by four-fold.[65] From the crystal structure of AT-FXa-pentasacchride (PDB ID: 2GD4) it was determined that FXa docks on to the front of AT allowing the reactive center loop (RCL) of AT to approach the active site of FXa, which is promoted by long heparin.[66] Previous mutagenesis studies identified Tyr-253 and Glu-255 of AT is crucial for interacting with the autolysis loop of FXa. The FXa residues Glu-37, Glu-39 and Arg-150 are involved in interacting with AT and Arg-150 was identified to be the most important residue since, the Ala substitution reduced the rate of inhibition by 10-fold.

1.4 Role of membranes in clotting cascade

1.4.1 Characteristics of Gla domains in mediating protein-membrane interactions in the clotting cascade

Membranes containing anionic phospholipids such as PS provide a procoagulant surfaces for the assembly of "extrinsic tenase", "intrinsic tenase" and the prothrombinase complex, essential for the initiation and propagation of the clotting cascade. Acceleration of the clotting reactions on the procoagulant membrane surfaces signify the regulatory role of phospholipids in the coagulation cascade.[67, 68] Clotting factors are equipped with unique membrane binding domains, which specifically recognizes PS. Cofactors FV and FVIII are part of the "intrinsic tenase complex" and "prothrombinase complex," and they have discoidin-type C2 domains that are known to bind to membrane with PS.[69, 70] Other procoagulant clotting factors FVII,FX,FIX,PT and anticoagulant clotting factors such as protein C, protein S and protein Z, belong to the family of vitamin K-

dependent proteins (VKD), that bind to membranes via their Gla domain. Gla-domains are highly conserved regions containing 9-13 Gla residues that are derived from the addition of a carbon di oxide to the γ-carbon of a Glu residue.[71, 72] Gla residues bind to multiple Ca^{2+} (and, in some cases Mg^{2+}) ions which play dual roles in proper functioning of the Gla domains. ^{13}C-NMR studies of selectively labeled polypeptides of the Gla domain in human protein C identified Gla residues 6, 16, 25 and 26 that coordinate with Ca^{2+} with high affinity Kd (<1.0mM) which were responsible for inducing correct conformation of the Gla domain by exposing the lipid binding sites involving Gla residues 7, 14, 19, 20 and 29, with lower affinity for Ca^{2+}.[73] Similar observations made in the FVIIa Gla-domain, the PT Gla-domain and protein C Gla-domain suggests that the role of tightly bound Ca^{2+} is to expose the hydrophobic residues in the ω-loop to establish hydrophobic interactions with the membrane and simultaneously express the lipid binding sites on the surface of the Gla domain.[74-76] Structural studies identified that in the PT Gla-domain, the carboxyl group of the serine interacted with Ca^{2+}-5, Ca^{2+}-6 and Gla residues 17 and 21 and the glycerophosphate backbone formed electrostatic interactions with basic residues Arg 16 and Arg 10.[77] Also, MD simulation studies of the FVII Gla-domain with membranes showed interactions between the PS headgroup and Ca^{2+}-7 and Ca^{2+}-8 and basic residue Arg-9 which coincides with the lipid binding site in PT Gla-domain.[78] Together, these studies provide evidences for a PS headgroup specific binding site present in the Gla domains and highlights the existence of several interactions such as calcium coordination, ionic interactions, van der Waals interactions and hydrophobic effects that are involved in the protein-lipid interactions in the Gla domains. Only at supraphysiological concentrations of >2mM, is Ca^{2+} able to saturate all the metal binding sites in the Gla domain. Therefore, under physiological conditions some metal binding sites are occupied by other divalent metal ion such as Mg^{2+} , which is present in plasma at about (0.6mM). Crystal structures of FVIIa/sTF in a physiologically similar conditions (2.5 mM Mg^{2+}/5 mM Ca^{2+}) show that the FVIIa Gla-domain at positions 1, 4 and 7 are occupied by Mg^{2+} and positions 2, 3, 6, 5 are occupied by Ca^{2+}.[79] Similar observations were made in Gla-domains of FIX and FX where some of the Ca^{2+} binding sites are replaced by Mg^{2+} at near physiological conditions.[80-82] Mg^{2+} occupancy of some of the metal binding site in Gla domains potentiates the ability of VKD proteins to bind membranes thereby enhancing the rate of clotting reactions.[80, 83-85] Interestingly, the Gla domains exhibit 90% sequence similarity but varying binding affinities ranging from 0.38-10 μM for L-PS containing membranes.[5] Slight differences among the Gla domains account for the wide range of binding

affinities. Absence of Gla-32 in protein C and FVII Gla domain inclines their preference towards PA over PS. Lack of Asp-34 from Gla domains of human protein Z and protein S in comparison to FX contributes towards the poor binding ability of these proteins.[86]

1.4.2 Interactions between FX Gla domain and anionic phospholipids.

The Gla domain of FX is 44 amino acid residues long and contains 11 Gla residues and mediates membrane interaction in a Ca^{2+} dependent manner. Chelation of Ca^{2+} by the Gla residues induces conformational change in the Gla domain which facilitates membrane binding.[87] Additionally, the first EGF like domain serves as a scaffold for proper folding of the Gla domain by utilizing a Ca^{2+} binding site as a hinge. [88-92] Comparison between Ca^{2+} free and Ca^{2+} loaded structures of the FX Gla-domain by homology modeling showed that solvent exposed Gla residues bind to Ca^{2+}, which exposes the hydrophobic residues Phe-4, Leu-5 and Val-8 in the ω-loop, to the solvent.[91] *In vitro*, Gla domainless FVIIa (GD-FVIIa) and soluble TF (sTF: amino acid residues 1-219) in presence of 1.3mM Ca^{2+}/0.5mM Mg^{2+} enhanced the rate of activation of full length FX but not for the Gla domainless FX (GD-FX), indicating that at near physiologic conditions Mg^{2+} occupies some of the Ca^{2+} binding sites in FX Gla-domain.[83] Although, the structural evidence for Mg^{2+} binding sites in FX Gla-domain is not yet published, three Mg^{2+} binding sites were identified in FIX-Gla domain. Due to high sequence similarity among the Gla domains of FIX and FX, these could also be potential Mg^{2+} binding sites in FX.[82] The crystal structure (PDB ID:1IOD) of FX Gla-domain bound to a FX-binding protein (X-bp) from a snake venom of *Denaigkistrodon acutus* was obtained with 7 Ca^{2+} ions ligated to the Gla residues, forming a patch of hydrophilic residues responsible for interacting with phospholipid headgroup and exposing hydrophobic residues to insert into the membrane. A novel Ca^{2+} binding site was observed in this structure involving Gla-32 and Gla-39 which is speculated to interact with FX cofactors and help in complex formation.[72] The Gla domain of FX binds to PS headgroups stereospecifically with a K_d of 0.380 ± 0.005μM.[5, 93] However, damage to the blood vessel expresses PE more abundantly along with PS on the cell surface membrane. Although, PE itself supports FX activation poorly, it synergizes with low amounts of PS molecules to enhance the rate of FX activation.[94, 95] The Anything But Choline (ABC hypothesis) for the binding of Gla domains to membranes proposed by our group, states that the membrane binding site or footprint for each FX-Gla domain consists of a limited number of PS molecules plus multiple PE molecules.[94] These findings indicate that the Gla domain of FX

has a unique PS binding site which specifically binds to PS headgroups in a lock and key fashion, while other membrane interactions can be fulfilled by the phosphate groups present in both PS and PE molecules. To understand the structural contributions of the FX Gla-domain towards high PS specificity, Molecular Dynamics (MD) simulation studies of the FX Gla-domain (PDB ID:1IOD) was conducted in presence of membranes containing 100% PS.[96] The membrane binding mechanism observed for FX-Gla domain in the MD simulation was in agreement with previous biochemical literature.[74, 77, 91] Most importantly, this study proposed two potential PS binding site in FX-Gla domain involving 1) PS, GLA19, Ca-6 and Ca-7; 2) PS, GLA29, GLN10, and Ca-1.[96] Gla-32 in FX-Gla domain also interacted with the amino group of PS molecule could potentially contribute towards PS specificity since it is absent in the Gla domain FVII and protein C, which bind to PS relatively weakly. A potent activator of FX derived from the venom of Russell's viper (RVV-X) binds to the Gla domain in presence of Ca^{2+} and prevents FX from binding the membrane surfaces.[97] RVV-X is a 57kDa metalloproteinase comprised of a heavy chain and a light chain and activates FX by cleaving the Arg194 and Ile195 bond like FVIIa.[98] The crystal structure of RVV-X (PDB:2E3X) when superimposed on the crystal structure of X-bp (PDB: 1IOD) showed the hydrophobic residues in X-bp that recognizes FX-Gla domain via the hydrophobic residues in the ω-loop are also conserved in RVV-X.[99] Hence, the FX-Gla domain is involved in crucial protein-protein and membrane-protein interactions required for proper functioning of the clotting cascade.

Chapter 2 Stoichiometric Analysis Reveals a Unique Phosphatidylserine Binding Site in Coagulation Factor X[a]

2.1 Introduction

The anionic phospholipid, phosphatidylserine (PS), is essential for reversible membrane binding of a number of clotting proteins.[100] Indeed, seven clotting proteins bind to PS-containing membranes via their γ-carboxyglutamate (Gla)-rich domains.[100] The surfaces of healthy, resting cells are anticoagulant because PS and phosphatidylethanolamine (PE) are sequestered to the inner leaflet of the plasma membrane, with phosphatidylcholine (PC) and sphingomyelin being the most abundant phospholipids in the outer leaflet.[101] Cellular injury or platelet activation leads to loss of membrane asymmetry and externalization of PS and PE, thus creating binding sites for clotting proteins.[100]

Artificial membranes containing PS dramatically enhance many clotting reactions, with maximal rates seen with 20-40% PS.[102, 103] However, mammalian plasma membranes typically have no more than about 10% PS, while the relatively more abundant glycerophospholipids, PC and PE, account for about 40% and 28%, respectively of the phospholipid content.[104, 105] Clotting reactions on liposomes with high PS content are therefore conducted under conditions far from the true physiological membrane composition. In 1994, Smirnov and Esmon reported that PE synergizes with PS to promote factor Va inactivation by activated protein C,[106] a finding that was subsequently extended by us and others to show that the presence of PE allows as little as 3 to 5% PS to support maximal rates of factor X (FX) activation by the tissue factor/factor VIIa complex,[95] prothrombin activation by the FXa/factor Va complex,[107] and factor VIII binding to membranes.[108] These low PS percentages are much closer to those found in plasma membranes, suggesting that

[a] This chapter has been adapted from a research article published in the Journal of Thrombosis and Haemostasis and used in accordance with the publisher's copyright privileges for publication in a dissertation thesis. Full citation: Paul D, Morrissey JH. Stoichiometric analysis reveals a unique phosphatidylserine binding site in coagulation factor X. J Thromb Haemost. 2021 Dec 11. doi: 10.1111/jth.15620.

the ability of PS/PE synergy to promote membrane binding by clotting proteins has physiologic significance.

In quantitative binding experiments using Nanodiscs of varying PS/PC composition, we previously showed that a membrane binding site for FX consists of 6 to 8 PS molecules, presumably clustered together via contact with the Gla domain.[109] We examined the mechanism of PS/PE synergy and found that almost any phospholipid tested (except PC) synergizes with PS to promote FX activation by the tissue factor/factor VIIa complex.[110] This led us to propose what we termed the Anything But Choline (ABC) hypothesis, which states that Gla domains bind to membranes via a limited number of "PS-specific" interactions that are satisfied only by PS, plus multiple "phosphate-specific" interactions that are satisfied by the far more abundant PE.[110] The idea is that a total of about 6 to 8 PS + PE molecules collaborate together to create a single FX binding site. Since structural details for Gla domain/membrane interactions are lacking, we felt it would be an important step forward to determine the minimum number of PS molecules that can constitute a FX binding site in the presence of excess PE. We hypothesized that this number would be an integer, and furthermore, that it could be as low as one PS-specific binding site per Gla domain. Accordingly, we now report the results of quantifying the stoichiometry of FX binding to Nanodiscs with a low number of PS molecules per disc and increasing PE content.

2.2 Materials

Phospholipids were from Avanti Polar Lipids (Alabaster, AL), as follows: PC, 1-palmitoyl-2-oleoyl-*sn*-glycero-3-phosphocholine; PS, 1-palmitoyl-2-oleoyl-*sn*-glycero-3-phospho-L-serine; and PE, 1,2-dioleoyl-*sn*-glycero-3-phosphoethanolamine. Human FX was from Haematologic Technologies (Essex Junction, VT). Membrane scaffold protein (MSP1D1) was expressed and purified as described.[111]

2.3 Methods

Nanodiscs were prepared by self-assembly reactions followed by purification as described,[112] using varying ratios of PC, PS and PE with MSP1D1. Phospholipid concentrations in samples of purified Nanodiscs were quantified by measuring total phosphate after complete hydrolysis,[113] while MSP1D1 protein concentrations were determined by A_{280} (extinction coefficient: 21,000 M^{-1} cm^{-1}).

Assuming two copies of MSP1D1 per Nanodisc,[112] the ratio of the molar concentration of phospholipid to MSP1D1 represents the number of phospholipid molecules per leaflet. This ratio was used to calculate the molecular mass (MW) of the entire Nanodisc from the MW of MSP1D1 (24.6 KDa) and the component phospholipids. Table 1 gives calculations for a typical set of Nanodisc preparations in this study.

FX binding to Nanodiscs of varying phospholipid composition was quantified via Surface Plasmon Resonance (SPR) as described,[109] using a Biacore T-200 instrument (Cytiva, formerly GE Healthcare). Briefly, Nanodiscs were immobilized by flowing in Loading Buffer (20 mM HEPES pH 7.4, 100 mM NaCl, 0.02% sodium azide) over Ni-NTA Series S Sensor chips and recording the net change in response units (RU) due to Nanodisc immobilization (RU_{ND}). For most experiments, this was about 770 to 1390 RU. Increasing FX concentrations were then flowed over Nanodisc-containing sensorchips at 30 μL/min in Loading Buffer plus 5 mM $CaCl_2$ and 0.2% bovine serum albumin. The maximal steady-state RU level was recorded at each input FX concentration (RU_{FX}), then divided by RU_{ND} to yield the RU_{FX}/RU_{ND} ratio (from which background binding to a parallel flow cell with 100% PC Nanodiscs was subtracted). Binding isotherms were generated by plotting RU_{FX}/RU_{ND} versus FX concentration, to which the single-site ligand binding equation (Equation 1) was fitted using Graph Pad Prism 8.0:

$$(1) \quad RU_{FX}/RU_{ND} = (B_{max} * x)/(K_d + x)$$

where B_{max} is the calculated maximal RU_{FX}/RU_{ND} ratio at saturation, x is the FX molar concentration, and K_d is the equilibrium dissociation constant. Phospholipid bilayers and proteins have equivalent refractive indices in solution.[114, 115] Therefore, by utilizing B_{max} from Equation 1, we calculated the number of FX molecules bound per membrane leaflet (N_{FX}) at saturation as shown in Equation 2:

$$(2) \quad N_{FX} = ((B_{max})*(MW_{ND}/MW_{FX}))/2$$

in which MW_{ND} is the MW of the Nanodisc, MW_{FX} is the MW of human FX (58.9 kDa), and division by 2 reflects two membrane leaflets per Nanodisc.

2.4 Results

Our goal was to determine the minimum number of PS molecules required to bind a FX molecule on nanoscale membrane bilayers in the presence of excess PE. We reasoned that limiting PS would minimize steric hindrance between bound FX molecules at saturation. We previously found that 100% PS Nanodiscs could bind 8.4 FX molecules per bilayer, which is close to the theoretical maximum number of Gla domains that could occupy the bilayer surface (about 10 FX Gla domains, based on cross-sectional area).[109] We therefore considered creating Nanodiscs with 10% PS. Given that Nanodiscs typically have 50 to 60 phospholipid molecules per leaflet, this should result in Nanodiscs with about 5 to 6 PS molecules per leaflet. Thus, if the minimum number of PS molecules that constitutes a FX binding site in the presence of excess PE turned out to be one, we would expect approximately 5 to 6 FX molecules bound per leaflet at saturation, which is less than the maximal packing of bound FX molecules previously measured on Nanodiscs. If the minimum number of PS molecules necessary to constitute a FX binding site (in the presence of excess PE) were greater than one, then we would expect even fewer FX molecules bound per leaflet at saturation.

Accordingly, we prepared Nanodiscs with 10% PS and increasing PE content (20, 40 or 60% PE, with the balance being PC). As a comparator, we prepared Nanodiscs with 50% PS but no PE (balance = PC). After carefully quantifying the phospholipid and MSP1D1 content of these preparations, we calculated the number of phospholipid molecules per leaflet and MW of each Nanodisc preparation (typical results in Table 2.1). The calculated numbers of PS molecules per Nanodisc were within the predicted range of 5 to 6 per leaflet. Note that these calculations assume that the PS content of Nanodiscs reflects the input PS content. We previously quantified this using ^{3}H-labeled PS and showed that the final PS content faithfully recapitulated the percent PS in self-assembly reactions, over a wide range of input PS contents.[109]

Table 2.1 Calculations for a typical set of Nanodisc preparations used in this study

Nanodisc lipid composition	Phospholipid [μM]*	MSP1D1 [μM]*	Phospholipid molecules/leaflet†	N_{PS}‡	MW_{ND} [kDa]
100% PC	550	9.59	57.4	0	136
50% PS, 50% PC	640	10.6	60.4	30.2	142
10% PS, 20% PE, 70% PC	680	11.9	57.1	5.71	136
10% PS, 40% PE, 60% PC	542	9.92	54.6	5.46	140
10% PS, 60% PE, 30% PC	451	9.31	48.4	4.84	122

*Phospholipid and MSP1D1 concentrations in purified Nanodisc preparations were quantified as described in Methods.
†Calculated as the ratio of the molar concentrations of phospholipid to MSP1D1.
‡N_{PS} (the number of PS molecules per leaflet) is the number of phospholipid molecules per leaflet multiplied by the fraction of the input phospholipid that was PS (i.e., 0, 0.5 or 0.1).

SPR-based binding analyses of FX with Nanodiscs

We next quantified FX binding to this range of Nanodisc preparations using SPR, with the resulting binding isotherms shown in Figure 2.1. Saturable, steady-state binding of FX was observed, as shown in a representative raw sensorgram of FX binding to Nanodiscs containing 10% PS, 20% PE, 70% PC Figure 2.1A. The binding affinities of FX to Nanodiscs containing 10% PS and varying PE Figure 2.1B were somewhat weaker than that observed with Nanodiscs containing 50% PS Figure 2.1C. Thus, the K_d value for FX binding to 50% PS Nanodiscs was 0.31 ± 0.14 μM, in close agreement with our previously reported K_d of 0.380 ± 0.005 μM for FX binding to such Nanodiscs.[116] For Nanodiscs with 10% PS and varying PE, the K_d values were: 1.57 ± 0.19 μM for 10% PS, 20% PE; 1.51 ± 0.54 μM for 10% PS, 40% PE; and 1.28 ± 0.20 μM for 10% PS, 60% PE (compared graphically in Figure 2.1D).

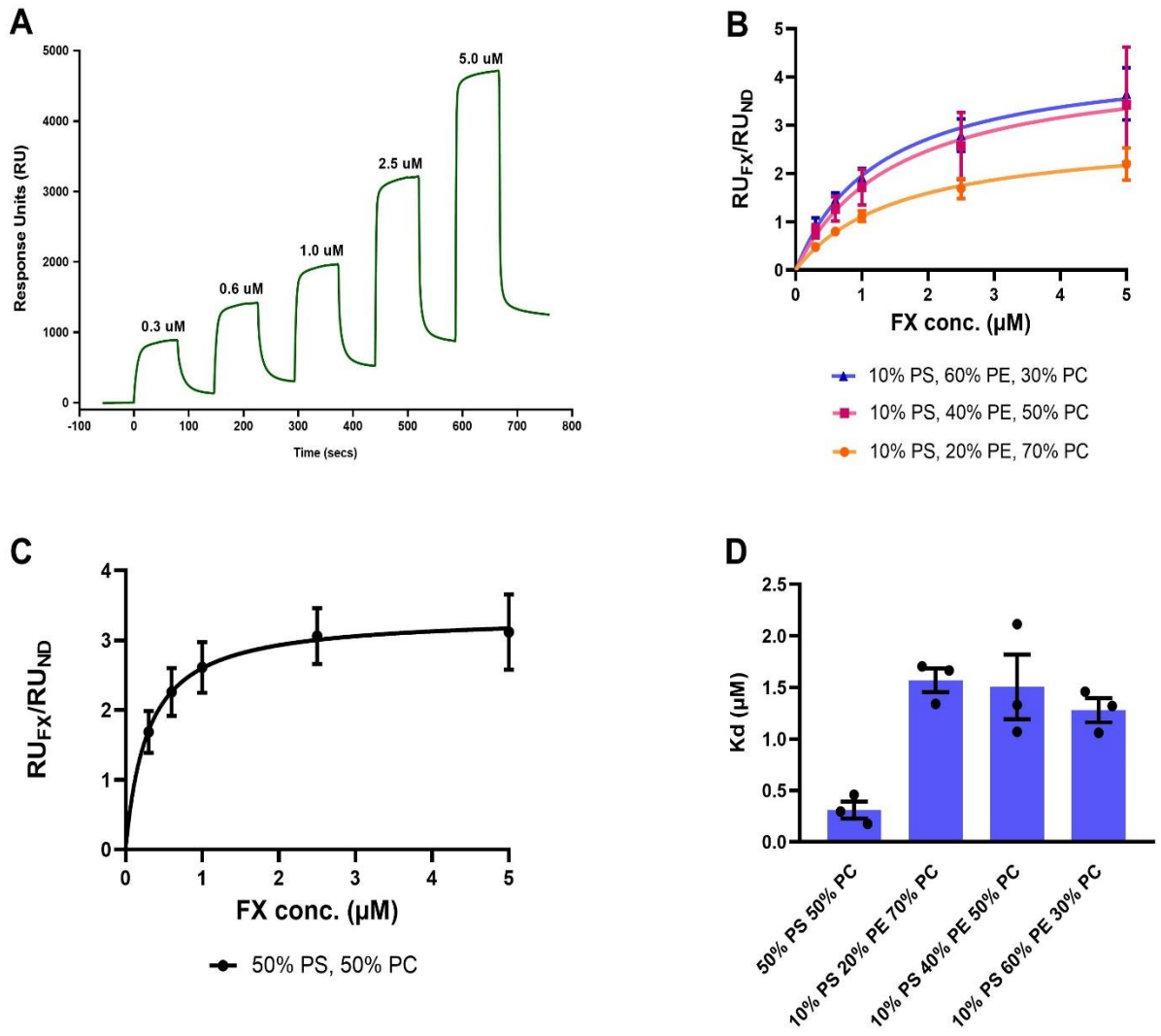

Figure 2.1 **Binding of FX to Nanodiscs of varying phospholipid composition, quantified by SPR**. (A) Raw sensorgram of FX binding to 10% PS, 20% PE, 70% PC Nanodiscs. (B) Binding isotherms of the association of FX with Nanodiscs of the following lipid compositions: 10% PS, 20% PE; 10% PS, 40% PE; and 10%PS, 60% PE. (C) Binding isotherm of the association of FX with Nanodiscs containing 50% PS. (In all cases, the balance is PC.) In panels B and C, RU_{FX}/RU_{ND} is plotted on the *y*-axis, which represents saturating RU values for FX binding (RU_{FX}) divided by the RU values for Nanodisc immobilization (RU_{ND}), after subtraction of background binding to a reference cell with 100% PC Nanodiscs. (D) Bar graphs of K_d values obtained by fitting equation 1 to the data in panels B and C. In panels B-D, error bars are standard error from three independent experiments.

Stoichiometry of FX binding

Table 2.2 summarizes the results of FX binding experiments to the range of Nanodiscs listed in Table 2.1, using three separate Nanodisc preparations for each experiment. For discs containing 50% PS, 50% PC, we found one FX binding site per 7.53 ± 1.3 PS molecules, in good agreement with our previous determination of one FX binding site per 7.97 PS molecules using Nanodiscs composed of binary mixtures of PS and PC.[109] When we examined FX binding to Nanodiscs containing 10% PS and varying PE, we found that the number of PS molecules per FX binding site decreased from 1.73 ± 0.4 with 20% PE down to 1.05 ± 0.2 with 60% PE.

Table 2.2 Stoichiometry of FX binding to Nanodiscs

Nanodisc lipid composition	**N_{PS}***	**N_{FX}†**	**N_{PS}/N_{FX}**
50% PS, 50% PC	30.4 ± 2.7	4.09 ± 0.4	7.53 ± 1.3
10% PS, 20% PE, 70% PC	5.31 ± 0.6	3.13 ± 0.6	1.73 ± 0.4
10% PS, 40% PE, 50% PC	4.74 ± 0.6	4.60 ± 2.0	1.16 ± 0.4
10% PS, 60% PE, 30% PC	4.64 ± 0.5	4.50 ± 0.7	1.05 ± 0.2

*N_{PS}, number of PS per leaflet.
†N_{FX}, number of FX molecules bound per leaflet at saturation.
Data are mean ± standard error; n = 3.

2.5 Discussion

These results indicate that the FX Gla domain requires just a single PS molecule to bind to membranes in the presence of excess PE, consistent with the ABC hypothesis[110] and extending it to state that there is only one truly PS-specific binding site in the FX Gla domain. Membranes consisting of binary PE/PC mixtures do not appreciably support FX binding or FX activation by the tissue factor/factor VIIa complex,[95, 110] which is also consistent with the notion that at least one PS molecule is required to create a Gla-domain binding site on the membrane, even in the presence of a large excess of PE.

Although there is weak but detectable binding of FX to PE/PC discs,[117] we chose to subtract background binding from 100% PC discs instead of PE/PC discs for the following reason. Nanodiscs with 10% PS, 60% PE, 30% PC have 48.4 phospholipids per leaflet (Table 1), which translates to 4.84 PS molecules and 29.0 PE molecules per leaflet. For such discs, we quantified 5.19 FX molecules bound per leaflet at saturation, meaning one FX molecule bound per 0.93 PS

+ 5.60 PE molecules (= 6.53 non-PC phospholipid molecules). As discussed above, one FX molecule binds for every 6 to 8 non-PC lipids, so it follows that virtually all the PE molecules are engaged with FX when it binds at saturation to these discs. Since there should be insufficient free PE molecules left to create another FX binding site under such conditions, we did not subtract FX binding to 60% PE, 40% PC discs.

We currently lack direct structural information on how Gla domains bind to membranes, although molecular dynamics simulations of Gla domain binding to PS-containing bilayers have provided tantalizing clues.[110, 118, 119] These simulations show Gla domains interacting with PS headgroups in multiple ways, sometimes involving just one charged group on the PS headgroup (such as the carboxylate or the phosphate), and other times involving interactions between multiple atoms in the PS headgroup and a combination of amino acid residues and bound Ca^{2+} in the Gla domain. Interestingly, binding of Gla domain-containing proteins to membrane surfaces requires PS with a headgroup composed of L-serine, not D-serine.[100, 110] This suggests that this one truly PS-specific binding site in the FX Gla domain is likely to bind the PS headgroup in a stereospecific manner, although this idea was not tested specifically in the present study. It will be interesting to further identify and characterize the unique PS binding site in the FX Gla domain, perhaps by mutagenesis or structural studies.

Chapter 3 Characterization of Factor X Gla-Domain Residues Critical for Initiation of the Clotting Cascade

3.1 Introduction

The first step towards achieving hemostasis is the activation of coagulation factor X (FX) by tissue factor (TF) and factor VIIa (FVIIa), thereby initiating the blood clotting cascade. Membranes containing negatively charged phospholipids such as phosphatidylserine (PS), promotes the assembly of the (TF/FVIIa) complex and simultaneously enhances the rate of FX activation by a 1000-fold.[30] While TF is an integral membrane protein, FVIIa and FX are soluble in nature. The N-terminal γ-carboxyglutamate-rich domain also known as the Gla domain of FVIIa and FX enables reversible transient protein-membrane interactions for the successful generation of activated FX (FXa). In 1996 Huang et al. observed 60-fold slower FX activation rates upon deletion of the Gla-domain from FX compared to FVIIa[24], necessitating characterization of the molecular interactions of FX Gla-domain critical for the initiation of the clotting cascade.

The FX Gla-domain contains 11 vitamin K dependent post-translationally modified γ-carboxylated glutamate residues whose side chains carry a charge of -2 and form coordination complexes with Ca^{2+} or Mg^{2+} ions to interact with PS containing membranes.[120] The crystal structure of the FX Gla-domain provides insight into the possible mechanism of the protein-membrane interaction mediated by the FX Gla-domain.[72] In presence of seven Ca^{2+} ions the FX Gla-domain folds properly, which exposes the hydrophobic residues in the ω-loop. These hydrophobic residues enable the FX Gla-domain to penetrate the phospholipid bilayer, thereby bringing the Gla residues near the PS headgroups on the membrane surface. TF residues Lys165 and Lys166 are located near the membrane and form part of the substrate recognition site for FX, also known as the "TF exosite". Mutating these two residues reduced FX activation rates by 80-85%.[23] Further, both wild-type and double mutant (Lys165A and Lys166A) TF supported same initial rates in presence and absence of membranes for Gla-domainless FX (GDFX).[24] Additionally, FVIIa poorly activated GDFX in solution as compared to wild-type FX.[30] These

studies are consistent with the importance of the FX Gla-domain in both membrane-protein and protein-protein interactions but they remain incompletely characterized.

Current structure biology techniques are limited and unable to fully capture the dynamic interactions between FX Gla-domain and the TF/FVIIa complex on membrane surfaces. Therefore, to unravel these complex interactions at the atomic level, *in silico* molecular dynamics (MD) simulation of the TF/FVIIa:FX ternary complex in solution were performed by two research groups from North Carolina Chapel Hill and Scripps Research Institute.[18, 19] Since the *in silico* models were designed based on previous structure studies of sTF bound to FVIIa [121, 122] in two different orientations, it presents a conflict in the FX Gla-domain residues predicted to interact with the TF/FVIIa complex residues. Therefore, a clear picture of FX Gla-domain interactions with the TF/FVIIa complex at the molecular level is yet to emerge.

In 2017 Muller et al., published a detailed analysis of the residues in FX Gla-domain that engaged with the PS headgroups in an all-atom MD simulation study.[96] In the present study, we mutated the FX Gla-domain residues predicted to have the longest contact time with PS headgroups to identify their contribution to protein-membrane and protein-protein interactions with the TF/FVIIa complex. We tested the influence of the mutants on the rates of FX activation by TF/FVIIa complex in presence and absence of the membranes. Additionally, binding studies with membranes were conducted to tease out the FX Gla-domain residues involved in membrane specific interactions. Combination of these studies allowed us to characterize the complex molecular interactions of the FX Gla-domain residues crucial for initiation of the clotting cascade.

3.2 Materials

Materials used in this study are as follows: 1-palmitoyl-2-oleoyl-*sn*-glycero-3-phosphocholine (POPC) and 1-palmitoyl-2-oleoyl-*sn*-glycero-3-phospho-L-serine (POPS) from Avanti Polar Lipids (Alabaster, AL); methoxycarbonyl-D-Nle-Gly-Arg-pNA acetate salt (FXa substrate) from Bachem (Bubendorf, Switzerland); recombinant human FVIIa from American Diagnostica (now Sekisui Diagnostics); Human FX wild type (FX-WT) and FXa from Hematologic Technologies (Essex Junction, VT); PureYield™ Plasmid Midiprep System from Promega (Madison,WI); Q-5® Site-directed mutagenesis kit from New England Biolabs (Ipswich,MA); Lipofectamine 2000 and Opti-Mem™ reduced serum media from Thermo Fischer (Waltham,MA); 500 mL DMEM

(Dulbecco's Modified Eagle's Medium)/Hams F-12 50/50 Mix from Corning® (Corning, NY); Vitamin K1 from Phytonadione, Henry Schein Medical (Melville, NY); Matched-Pair Antibody Set for ELISA Human FX Antigen from Enzyme Research Laboratory (South Bend, IN); Custom DNA oligonucleotides were synthesized by Integrated DNA Technologies (IDT, San Jose, CA, USA); His Ni-NTA (nitrilotriacetic acid) Resin, succinimidyl-[(N-maleimidopropionamido)-hexaethyleneglycol]ester (SM(PEG)$_6$), AminoLink™ Plus Immobilization Kit, Pierce BCA protein assay kit, and StartingBlock™ (PBS) Blocking Buffer were purchased from ThermoFisher Scientific (Waltham, MA, USA).

3.3 Methods

Production of recombinant FX Gla-domain mutants

FX-WT encoded in pcDNA3.1(+) expression vector from Genscript Biotech (Piscataway,NJ) was used as a template to generate 11 FX Gla-domain mutants: Gla-7 ([b]γ7D), Lys-9 (K9Q), Lys-10 (K10Q), Gla-14 (γ14D), Arg-15 (R15Q), Gla-19 (γ19D), Gla-20 (γ20D), Arg-28 (R28Q) and Gla-32 (γ32D), (γ32A) by site-directed mutagenesis. 0.5 µg of each plasmid was transfected with Lipofectamine 2000 in HEK293/VKOR cells (HEK 293 cells that overexpress vitamin K 2,3-epoxide reductase C1 expression vector, a kind gift from Darrell Stafford). Transfected HEK293/VKOR cells were selected against 600µg/ml G418 by Fischer scientific (Waltham,MA) and monoclonal stable cell lines were generated by serial dilution method. Expression of FX Gla-domain mutants were carried out in cell factories (Corning HYPER*flask* M Cell Culture Vessel) in DMEM media supplemented with L-Glutamine, 15 mM HEPES, 10 µg/ml vitamin K1, 2 µg/ml of Puromycin and 400µg/ml of G-418. Expression of recombinant FX Gla-domain mutants were confirmed by FX-Enzyme Linked Immunosorbent Assay (ELISA). Recombinant FX Gla domain mutants with HPC4 tag were purified by affinity chromatography as described previously.[123] Subsequently, fully carboxylated FX Gla domain mutants were purified by anion exchange chromatography column packed with Mono Q beads in AKTA Pure (Cytiva, Marlborough, MA).

[b] The Gla residues are denoted by the Greek letter γ.

FX activation assay in solution

Soluble TF (sTF) was expressed in *Escherichia coli* and purified as described previously.[124] The initial rates of FX activation by sTF/FVIIa were measured by discontinuous (two-stage) assay in 96-well microplates. In the first stage, 0.5 µM of FX-WT and FX Gla-domain mutants were added to 1µM sTF, 40 nM FVIIa and 5mM Ca^{2+} in HBSA (20 mM HEPES at pH=7.4, 100 mM NaCl and 0.1% BSA). 10µl aliquots of the reaction mixture were taken at every 5-minute time interval and added to 80µl of 10mM EDTA to quench the reaction. In the second stage, after 15 mins, 0.5 mM of FXa substrate was added to spectrophotometrically measure the amount of FXa generated by sTF/FVIIa at A_{405} in Spectramax 96-well spectrophotometer by Molecular Devices (San Jose, CA). A standard curve of FXa at varying concentration corresponding to the rates of chromogenic substrate hydrolysis was utilized for quantifying the amount of FXa generated by sTF/FVIIa.

FX activation assay in PC/PS membranes

Recombinant human membrane anchored TF (residues 3-244) was expressed in *Escherichia coli* and purified as described previously.[95, 125] TF was incorporated in liposomes made of 20% POPS and 80% POPC as described previously[126] using Biobeads SM-2 and 20mM sodium deoxycholate from Sigma Aldrich (St. Louis, MO). The initial rates of FX activation by TF/FVIIa on membrane surfaces were measured by continuous assay in 96-well microplates as described previously[125], typically using 0.6 nM TF, 10 µM lipids, 3-96 pM FVIIa, 30 nM FX and recombinant FX Gla-domain mutants.

Data processing for FX activation assays

The initial rates of FX activation by TF/FVIIa complex in solution were measured by two-stage discontinuous assay. In the final stage, the colorimetric change observed after cleavage of FXa substrate at 405 nm was recorded as milli-OD/min to generate a linear plot. The slope of various plots were determined to quantify the relative rates of FX activation in solution. Data reported in this study are the slopes of FX mutants normalized by the slopes measured for FX-WT run in parallel in an individual experiment.

The initial rates of FX activation by TF/FVIIa complex on membranes were measured by continuous assay where the colorimetric change observed after cleavage of FXa substrate at 405

nm was recorded as milli-OD/min vs min which generated a hyperbolic curve. This was fitted to the quadratic equation $y = A + Bx + Cx^2$ in SoftMax Pro 7.0.3. which was used to calculate the second order derivative to quantify the initial rates of FX activation of both wild-type and mutants. Data reported in this study for the initial rates of FX mutants were normalized by the initial rates observed for FX-WT.

DNA-Tagged Nanodisc preparation and purification

Custom DNA oligoes conjugated to $SM(PEG)_6$ in 1:10 molar ratio in PBS-8(+) (10 mM PBS, 3 mM EDTA, pH 8) and 20% DMSO for 1 hour at room temperature. His-Tagged Membrane Scaffold Protein (MSP1D1 with D73C mutation) was expressed and purified as described previously.[127] At molar ratio of 10:5:1 of sodium cholate to MSP1D1 D73C to TCEP in PBS-6.5(+) buffer was incubated for 30 mins. Conjugated DNA after dialysis in PBS-6.5(+) buffer was incubated with reduced MSP1D1 D73C for 2 hours or overnight at 4°C and excess DNA was removed by Ni-NTA purification. Conjugated MSP was purified by using DNA columns generated with DNA oligo complements and the AminoLink™ Plus Immobilization Kit in TBS (20 mM Tris, 100 mM NaCl, 0.5 mM EDTA, 0.01% NaN_3, pH 7.4) buffer. Nanodiscs containing 50% POPS and 50% POPC were assembled with DNA-tagged MSP1D1 as described previously.[128]

Binding studies of FX Gla-domain mutants with DNA-Tagged Nanodiscs

The binding studies were carried out in Maverick M1 optical scanning instrumentation and microring resonator sensor chips functionalized with complement DNA by Genalyte, Inc. (San Diego, CA)[129]. The microring resonator is advantageous to test the biological and technical replicates in a single experiment with ~20ug of protein. Upon binding the silicon photonic microring resonator detects changes in the refractive index near the surface which results in a shift in the resonant wavelength. Like SPR it allows us to monitor real-time binding with label free samples. The DNA-Tagged Nanodiscs[130] were loaded at 10ul/min flow rate in TBS buffer with 2% BSA, such that there were 2-3 biological replicates of 50% POPS and 50% POPC Nanodiscs and 100% POPC Nanodiscs (control) in clusters of 4 technical replicates (n=8-12) (Figure S1). Both FX-WT and recombinant FX Gla domain mutants were flowed at 10µL/min flow rate over the Nanodiscs at 100 nM, 250 nM, 750 nM, 2.5µM and 5µM concentrations except recombinant FX Gla-domain K9Q and K10Q were flowed at 100nM, 250nM, 750nM, 2µM and 4µM as per the protein availability. The bulk non-specific binding and temperature fluctuations were corrected by

subtracting the response of ssDNA control. To account for the differences in surface coverages for individual microring the following equation 1, where $\Delta pm_{Protein}$ is the relative shift response during the protein titration, $M_{w,Protein}$ is the molecular weight of the titrated protein, $\Delta pm_{Nanodisc}$ is the quantified loading of Nanodisc, and $M_{w,Nanodisc}$ is the molecular weight of the Nanodisc was used.

$$Protein\ per\ leaflet = \left(\frac{\Delta pm_{Protein}}{M_{w,Protein}}\right)\left(\frac{M_{w,Nanodisc}}{\Delta pm_{Nanodisc}}\right)\left(\frac{1}{2}\right)$$

The binding curves were generated by plotting the relative shift in protein per leaflet at the equilibrium versus the protein concentration. These were fitted to the following equation 2 to determine the K_d dissociation constant values and FX was the titrated protein concentration. The data analysis was performed using a custom R script in R studio.

$$Protein\ per\ leaflet = Protein\ per\ leaflet_{max}\ \left(\frac{X}{K_d + X}\right)$$

Molecular Dynamics (MD) Simulation of FX Gla domain mutants in solution

All MD simulations were performed using NAMD2 [131] with CHARMM36 force fields [132, 133] and TIP3P water. Parameters of GLA residues were developed previously[78] with atom types renamed as appropriate for conversion from CHARMM27. Long-range electrostatic interactions were calculated using the particle mesh Ewald (PME) method [134]. Non-bonded interactions were calculated with truncation after 12 Å and a smoothing function started at 10 Å. SHAKE and SETTLE algorithms[135, 136] were applied to constrain bonded hydrogen atoms. Constant temperature was maintained at 310 K by Langevin dynamics with a damping coefficient of 1.0 ps^{-1}. Constant pressure was maintained at 1 atm using the Nosé-Hoover Langevin piston method[137]. All simulations were performed with a 2-fs timestep. WT and all mutant proteins were first energy minimized for 2,500 steps by using steepest descent algorithm and equilibrated for 50 ns with Cα atom harmonic restraints (k = 3 kcal mol^{-1} $Å^{-2}$). Three independent replicas of each protein system were then simulated without restraints for 250 ns. VMD[138] was used for visualization and analysis.

3.4 Results

Mutagenesis of FX Gla-domain residues predicted to interact with PS headgroup

To identify the FX Gla-domain residues critical for initiation of the clotting cascade, eleven residues in FX Gla-domain were mutated by site-directed mutagenesis studies. Membranes

containing PS dramatically increase the rates of FX activation by TF/FVIIa complex. Therefore, on the basis of the previous MD simulation study[96] we chose the Gla residues at positions 7, 14, 19, 20, 25 and 32 that interacted with the amino group of PS headgroup Figure 3.1 A and the positively charged residues at positions 9, 10, 15 and 28 that interacted with the phosphate group Figure 3.1B of PS headgroup. The different functional groups of PS headgroups are shown in Figure 3.1C.

Recombinant FX Gla-domain mutants were expressed in HEK 293 cells, and their structural stability was tested with MD simulation studies, where each mutant was equilibrated for 250ns in solution. The root mean square deviation (RMSD) in the C_α atom of the protein backbone was measured for FX-WT and eleven FX Gla-domain mutants. The RMSD values of the three replicas of each FX Gla-domain mutants and FX-WT are shown in Table S 3.1RMSD of FX Gla-domain mutants from FX-WT in solution

The following FX Gla-domain mutants, Gla-25 (γ25D), Gla-20 (γ20D) and Gla-32 (γ32D), listed in increasing order of their RMSD values with respect to FX-WT were predicted to destabilize the structure of the FX-Gla domain also shown in Figure 3.1C.

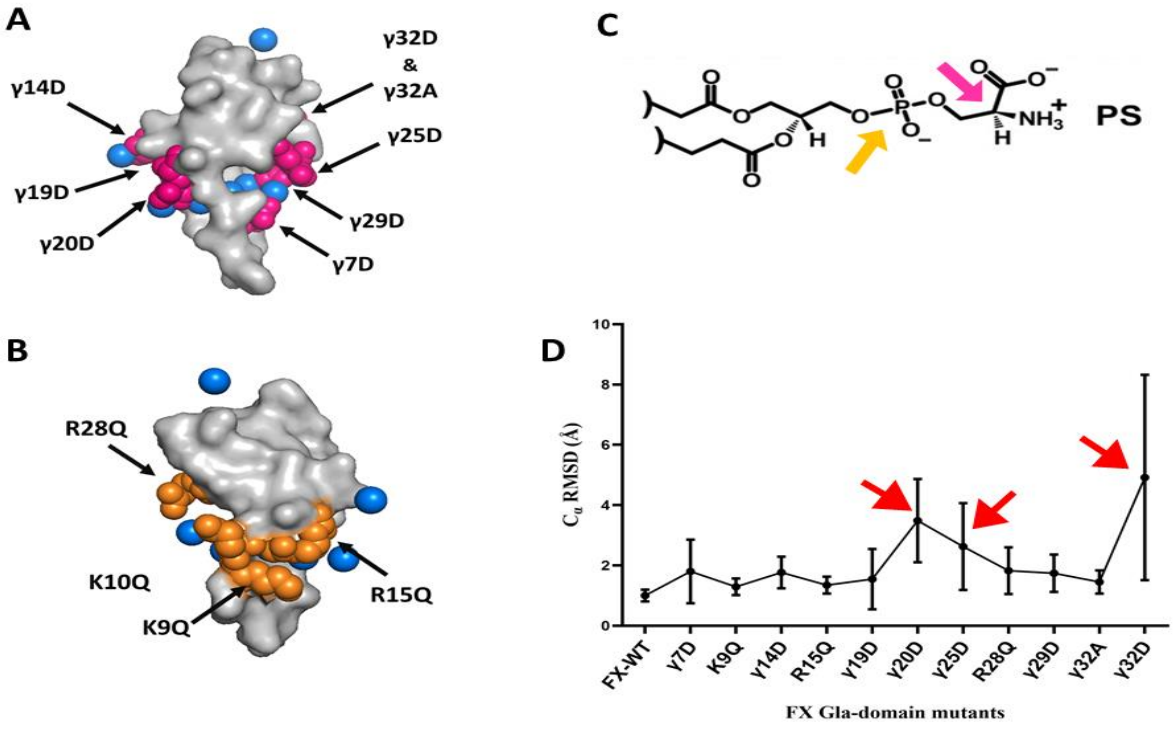

Figure 3.1 **FX Gla-domain residues selected for site directed mutagenesis and their effect on the stability of the FX Gla-domain.** Single point mutants generated for the negatively charged residues and positively charged residues in FX Gla-domain are highlighted in panel (A and B) respectively. Bovine derived FX Gla-domain structure was obtained from PDB: 1IOD, where Gln is present at position 10 instead of lysine and here we have adapted that for human FX Gla-domain. (C) Atomic structure of phosphatidylserine (PS) headgroup. Frequent interactions observed in previously published MD simulation studies between the residues in Panel A and the amino functional group of PS is denoted by a pink arrow and the residues in Panel B with the phosphate functional of PS group is denoted with the orange arrow. (D) MD simulation studies of FX Gla-domain mutants for 250ns in solution. Red arrows highlight the residues that affected the stability of the FX Gla-domain the most upon mutagenesis.

Influence of mutagenesis on rates of FX activation by TF/FVIIa complex in presence and absence of the membranes.

We hypothesized that the protein-protein interaction between FX and TF/FVIIa complex will not be affected upon mutating a single residue in the FX Gla-domain. To test our hypothesis, we measured the initial rates of FX activation by sTF/FVIIa in solution Figure 3.2 (B and C). The following FX Gla-domain mutants: Lys-9 (K9Q), Arg-15 (R15Q), Gla-25 (E25D), Gla-32 (E32D and E32A) and Arg-28 (R28Q) showed 30-40% higher rates of FX activation as compared to FX-

WT. While FX Gla-domain mutants, Lys-9 (K9Q) and Gla-19 (E19D) showed 15% less activation rates than FX-WT. Together, these observations indicate that mutagenesis of FX Gla-domain residues at positions 9, 10, 15, 19, 25, 28 and 32 have significantly less impact on the protein-protein interactions between FX and TF/FVIIa complex. However, we observed that mutagenesis of FX Gla-domain residues, Gla-7 (γ7D), Gla-14 (γ14D), Gla-20 (γ20D) and Gla-29 (γ29D) reduced the rates of FX activation by 50-80%. Thereby, showing that FX Gla-domain residues at positions 7, 14, 20 and 29 possibly play a significant role in mediating protein-protein interactions with the TF/FVIIa complex.

In physiology, FX activation by TF/FVIIa complex occurs on membrane surfaces containing negatively charged phospholipids such as PS. Previous studies from our group and others have shown that during the process of FX activation by TF/FVIIa complex, the FX Gla-domain engages with TF "exosite", FVIIa Gla domain and membrane surfaces.[23, 24, 29, 30] We hypothesized that measuring the rates of FX activation by TF/FVIIa complex on membranes would allow us to identify the FX Gla-domain residues involved in protein-protein as well as protein-membrane interactions during the initiation of the clotting cascade. The influence of mutagenesis on the rates of FX activation by TF/FVIIa complex on membranes containing 20% PS and 80% PC are shown in Figure 3.2 (E and F). The mutagenesis of the positively charged FX Gla-domain residues: K9Q, K10Q showed 30% decrease and R15Q, R28Q showed 40-50% decrease in the rates of FX activation. A contrasting observation was made in FXa generation upon the mutagenesis of the negatively charged Gla residues. We measured 90-95% lower FX activation rates in case of the following FX Gla-domain mutants: γ14D, γ19D, γ25D, γ32D and γ32A. Whereas no measurable rates of FXa generation by TF/FVIIa was observed in presence of the following mutants γ7D, γ20D and γ29D. Our results show that mutagenesis of the Gla residues severely impacts both protein-protein and protein-membrane interactions as compared to the positively charged FX Gla-domain mutants.

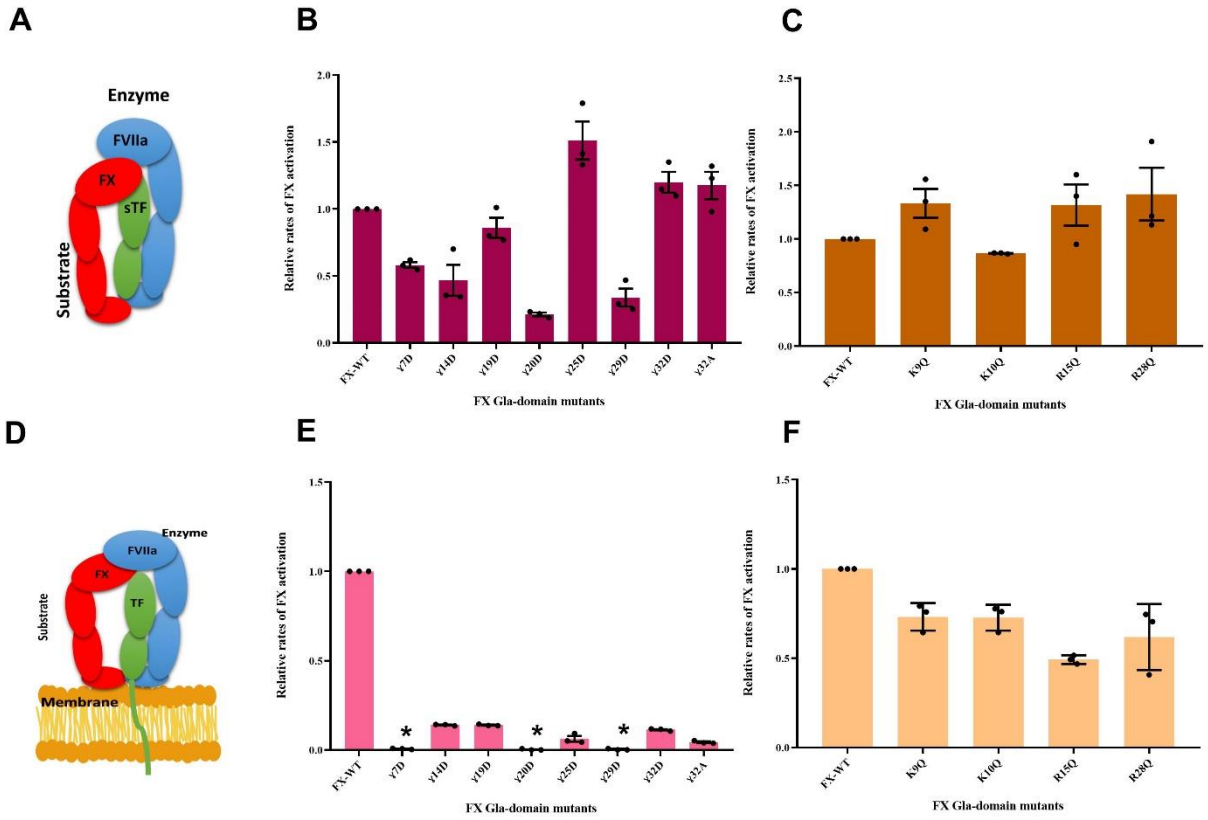

Figure 3.2 **Influence of mutagenesis on rates of FX activation in presence and absence of membranes.** (A) Cartoon representation of (A) FX activation by sTF and FVIIa complex in solution and (D) FX activation by TF/FVIIa complex on membranes. The impact of mutating negatively charged residues γ7D, γ14D, γ19D, γ20D, γ25D, γ29D, γ32D and γ32A on rates of FX activation in solution and on membrane surfaces are presented in panels (B and E) respectively. The impact of mutating positively charged residues in K9Q, K10Q, R15Q and R28Q on rates of FX activation in solution and on membrane surfaces are presented in panels (C and F) respectively. (B and C) Initial rates of FX activation by sTF and FVIIa and (E and F) the initial rates of FX activation by TF/FVIIa complex on 20% POPS and 80% POPC liposomes of FX Gla-domain mutants were normalized to FX-WT for each day. *<0.01 relative rates of FX activation were recorded. Data are represented as mean ± standard error N=3.

Impact of mutagenesis on binding ability of FX Gla-domain to membranes.

To identify the FX Gla-domain residues specifically involved in protein-membrane interaction we measured the binding affinities of FX Gla-domain mutants to DNA-Tagged Nanodiscs containing 50% PS and 50% PC. The DNA-tagged Nanodiscs were loaded on to the sensor surface to generate the array shown in Figure S 3.1. The array comprised of 2-3 biological replicate of 100% PC as a negative control and 50% PS 50% PC. Due to low binding levels of FX Gla-domain

mutants we here report the number of FX molecules bound per leaflet of 50% PS and 50% PC DNA-Tagged Nanodiscs using equation 1, summarized in Table 3.1. Binding affinities (K_d) were quantified by utilizing equation 2 summarized in Table S 3.2 The raw sensorgrams for FX-WT and each FX Gla-domain mutants and their respective binding isotherms are shown in Figure S 3.2. We quantified 4.7 ± 0.9 FX-WT molecules were able to bind with 50% PS and 50% PC DNA-Tagged Nanodiscs which lies within the range of our previously reported 7.53 ± 1.3 FX-WT molecules bound to 50% PS 50% PC Nanodiscs.[139] The difference is experimental setup of measuring the value of number of FX binding to 50% PS 50% PC Nanodiscs accounts for the variability in the two values. Among all the FX Gla-domain mutants only γ19D, K9Q and R15Q mutants demonstrated significant binding to the 50% PS containing DNA-Tagged Nanodiscs. We observed that these mutations reduced the number of FX molecules bound per leaflet approximately by 40-70%. For FX Gla-domain mutants γ14D and γ32D we observed <1 molecule bound per leaflet and for K10Q and R28Q nearly one molecule of FX was able to bind 50% PS and 50% PC membranes. For these residues minimal binding was observed in this study and are reported in the raw sensorgram in Figure S 3.2 (X and Z). Lastly, in the binding study of following FX Gla-domain mutants γ7D, γ20D, γ25D, γ29D and γ32A we recorded no response shown in Figure S 3.2 (O, R, S, T and V). This indicated that mutagenesis of these residues completely abolished the membrane binding capability of FX.

3.5 Discussion

The interactions of FX Gla-domain critical to the initiation of the clotting cascade are investigated here at the molecular level. We employed extensive mutagenesis studies to unravel the residues in the FX Gla-domain responsible for mediating protein-protein and membrane-protein interactions. Both protein-protein and membrane-protein interactions were impacted more upon mutating the Gla residues as compared to the positively charged residues in the FX Gla-domain. The higher impact on these interactions by the Gla residues can be attributed to their involvement to multiple interactions with the Ca^{2+} ions, amino and carboxylate functional group on the PS headgroup.

Previous MD studies identified that γ7 and γ20 interact with the Ca^{2+} ions that are responsible for the structural stability of the FX Gla-domain and furthermore, γ7 and γ29 engage in the longest

Table 3.1 Maximum number of FX molecules bound per leaflet of the DNA-Tagged Nanodiscs

	Protein	50% PS 50% PC
Negatively charged residues	FX-WT	4.7 ± 0.9
	γ7D	NA†
	γ14D	0.28 ± 0.06
	γ19D	2.2 ± 0.4
	γ20D	NA†
	γ25D	NA†
	γ29D	NA†
	γ32D	0.57±0.09
	γ32A	NA†
Positively charged residues	K9Q	1.2 ± 0.2
	K10Q	0.7 ± 0.2
	R15Q	1.9 ± 0.4
	R28Q	0.8 ± 0.1

NA†: The number of FX molecule bound per leaflet was not quantified due to poor or no binding.
Data are mean ± standard error N=3

contact time with the PS headgroup.[96] Not surprisingly, upon mutating the Gla residues at positions 7, 20 and 29 we also observed drastically reduced rates of FX activation in solution and in presence of the membrane by the TF/FVIIa complex and no saturable binding to membranes containing up to 50% PS. This would suggest that mutating γ7 and γ20 could result in improper engagement of FX with the TF/FVIIa complex. The MD simulation studies in solution of the FX Gla-domain containing the mutation of Gla→Asp at position 7, 20 and 29 performed here show no impact on the structural stability of the Gla domain in solution. A reasonable explanation for these observations would be that deleting one carboxylate group from γ7 and γ20 is still allowing γ7D and γ20D to engage with Ca^{2+} ion and maintain the structural integrity of the isolated FX Gla-domain in solution but in presence of TF/FVIIa complex and membranes these residues require the additional carboxylate group to mediate both protein-protein and membrane-protein

interactions. In FX-WT one carboxylate group for residue γ29 interacts with the amino group in the PS headgroup and the other one interacts with a lipid interacting Ca^{2+} ion[96]. As mentioned above among all the Gla residues, γ29 is involved in the second longest interaction time with PS, thus mutating γ29D leaves only one carboxylate group which is incapable of forming stable protein-membrane interactions, thereby resulting in poor rates of FX activation.

Since the ternary complex of TF/FVIIa with FX plays the important role of initiating the clotting cascade, two groups from North Carolina Chapel Hill and Scripps Research Institute docked FX on to the crystal structure of sTF/FVIIa complex, to identify the intermolecular interactions within the complex. In the Scripps model, γ14 participated in the ionic interaction with the Arg 36 residue of FVIIa Gla-domain.[20] Another study showed that mutating γ14 (Gla →Lys) reduced the K_d between FX and TF/FVIIa, which supports the idea of γ14 being involved in molecular interaction with TF/FVIIa complex.[140] In agreement with previous observations we also see here that mutating γ14D impacted both protein-protein and membrane-protein interaction of FX Gla-domain.

In the Scripps model γ32 formed an ionic interaction with TF exosite residue Lys 166. γ32 is not present in factor VIIa and Protein C, which are the only two vitamin-K dependent blood clotting factors that prefers to bind phosphatidic acid over PS, which supports the hypothesis that this residue is crucial for membrane binding.[116] Here we prepared two mutants γ32D and γ32A to fully probe the molecular interactions of this residue. Although, the MD simulation showed that mutating γ32 destabilized the isolated FX Gla-domain in solution, but we observed no effect on the rates of FX activation in solution by TF/FVIIa. In presence of membranes containing PS, the rates of FX activation by TF/FVIIa were reduced by 90-95%. With γ32D we observed poor binding, but no binding was observed with γ32A. These results indicate that γ32 is highly important for protein-membrane interaction since removal of one carboxylate group drastically impacts membrane binding but removal of both the carboxylate groups incapacitates FX binding. The experiments performed here cannot support the hypothesis of γ32 interacting with Lys 166 TF and future studies of reversing the charge on this residue can address this question. Mutating γ25D severely impacted the protein-membrane interactions of FX but not the protein-protein interactions which corroborates well with previous MD simulation studies by Muller et al.

We further mutated the positively charged FX Gla-domain residues at position 9, 10, 15 and 28 to a neutrally charged glutamine residue. Previous MD simulation studies by Muller et al., showed that these residues engaged in ionic interactions with either the negatively charged phosphate or carboxylate ion in the PS headgroup. Here we see that disrupting these ionic interactions were not extremely detrimental to FX binding to the membrane.

In conclusion, these results show that the FX Gla-domain residues engaging with the amino functional group of PS play a major role in the protein-membrane interactions critical for the initiation of the clotting cascade.

3.6 Supplementary figures and tables

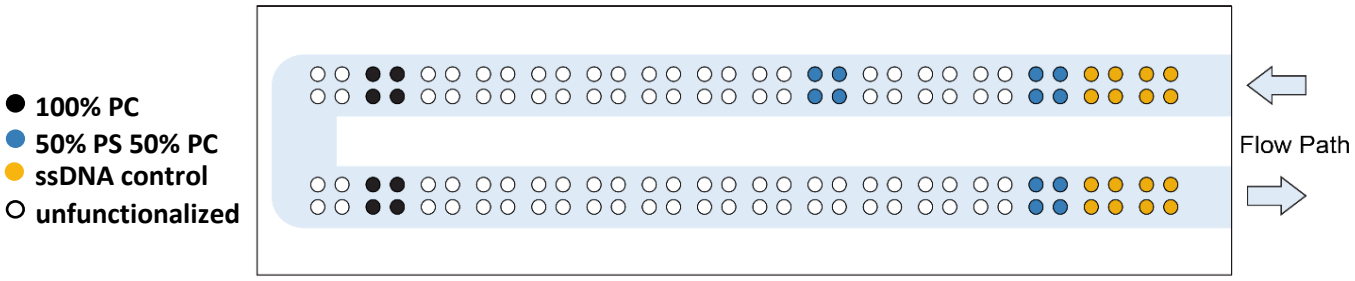

Figure S 3.1 **Sensor Chip Layout.** Light blue box represents the flow path for Nanodisc array titration, and the arrows indicate the U-channel setup utilized in this study. Flow loading was used to generate the array of 50% PS 50% PC (blue) to measure FX binding and 100 % PC (black), unfunctionalized microrings (white) and ssDNA (yellow) that act as negative controls. This allows 2-3 biological replicates with 4 technical replicates each for every Nanodisc (n = 8-12).

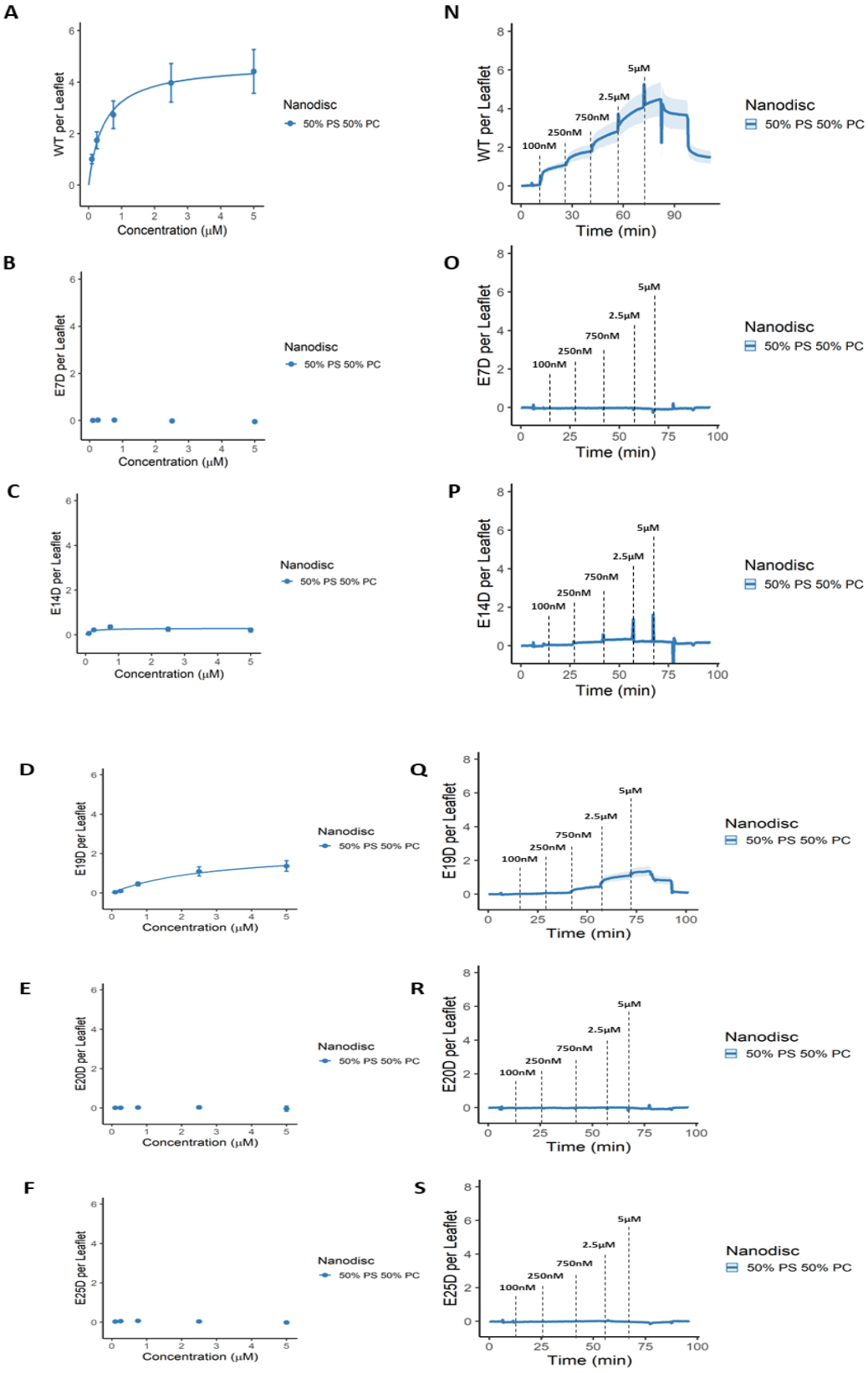
A
WT per Leaflet
Concentration (μM)
Nanodisc
50% PS 50% PC
N
WT per Leaflet
Time (min)
100nM
250nM
750nM
2.5μM
5μM
Nanodisc
50% PS 50% PC
B
E7D per Leaflet
Concentration (μM)
Nanodisc
50% PS 50% PC
O
E7D per Leaflet
Time (min)
100nM
250nM
750nM
2.5μM
5μM
Nanodisc
50% PS 50% PC
C
E14D per Leaflet
Concentration (μM)
Nanodisc
50% PS 50% PC
P
E14D per Leaflet
Time (min)
100nM
250nM
750nM
2.5μM
5μM
Nanodisc
50% PS 50% PC
D
E19D per Leaflet
Concentration (μM)
Nanodisc
50% PS 50% PC
Q
E19D per Leaflet
Time (min)
100nM
250nM
750nM
2.5μM
5μM
Nanodisc
50% PS 50% PC
E
E20D per Leaflet
Concentration (μM)
Nanodisc
50% PS 50% PC
R
E20D per Leaflet
Time (min)
100nM
250nM
750nM
2.5μM
5μM
Nanodisc
50% PS 50% PC
F
E25D per Leaflet
Concentration (μM)
Nanodisc
50% PS 50% PC
S
E25D per Leaflet
Time (min)
100nM
250nM
750nM
2.5μM
5μM
Nanodisc
50% PS 50% PC

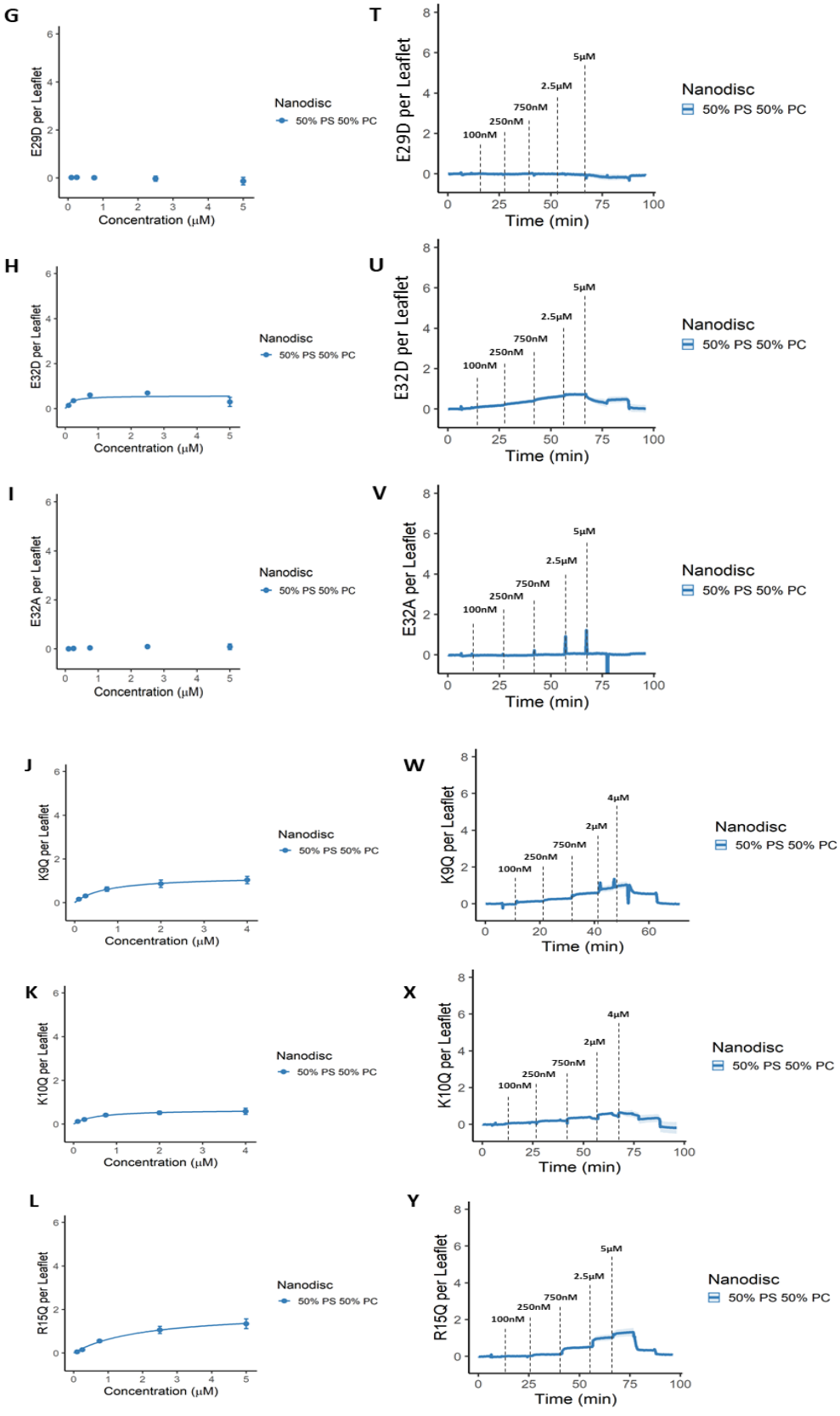
G
E29D per Leaflet
Concentration (μM)
Nanodisc
50% PS 50% PC
T
E29D per Leaflet
100nM
250nM
750nM
2.5μM
5μM
Time (min)
Nanodisc
50% PS 50% PC
H
E32D per Leaflet
Concentration (μM)
Nanodisc
50% PS 50% PC
U
E32D per Leaflet
100nM
250nM
750nM
2.5μM
5μM
Time (min)
Nanodisc
50% PS 50% PC
I
E32A per Leaflet
Concentration (μM)
Nanodisc
50% PS 50% PC
V
E32A per Leaflet
100nM
250nM
750nM
2.5μM
5μM
Time (min)
Nanodisc
50% PS 50% PC
J
K9Q per Leaflet
Concentration (μM)
Nanodisc
50% PS 50% PC
W
K9Q per Leaflet
100nM
250nM
750nM
2μM
4μM
Time (min)
Nanodisc
50% PS 50% PC
K
K10Q per Leaflet
Concentration (μM)
Nanodisc
50% PS 50% PC
X
K10Q per Leaflet
100nM
250nM
750nM
2μM
4μM
Time (min)
Nanodisc
50% PS 50% PC
L
R15Q per Leaflet
Concentration (μM)
Nanodisc
50% PS 50% PC
Y
R15Q per Leaflet
100nM
250nM
750nM
2.5μM
5μM
Time (min)
Nanodisc
50% PS 50% PC

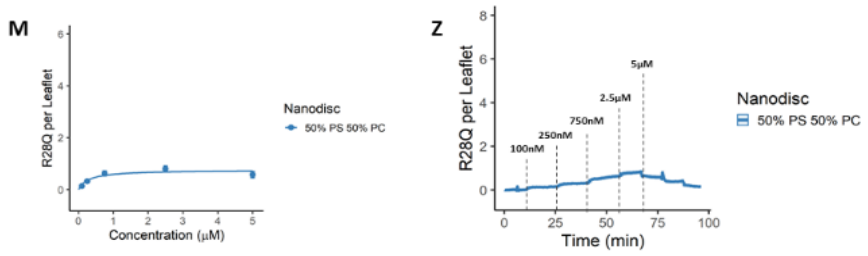

Figure S 3.2 **Titration of wildtype factor X (FX-WT) and FX Gla-domain mutant.** (**A-I**) Binding isotherms of FX-WT and mutants that target FX Gla residues γ7D, γ14D, γ19D, γ20D, γ25D, γ29D, γ32D and γ32A and **(J-M)** that target positively charged FX Gla-domain residues K9Q, K10Q, R15Q and R28Q. Normalized and 100% PC controlled FX titration from 100 nM to 5 μM of **(N-V)** FX-WT and Gla residue mutants **(W-X)** 100 nM to 4 μM of FX Gla-domain mutants K9Q and K10Q and **(Y-Z)** FX Gla-domain mutants R15Q and R28Q.The shaded ribbon shows the standard deviation of microrings (n = 8-12). The FX per leaflet values were calculated from equilibrated steps in the titration using the first calcium buffer step as a zero point and the binding isotherm was generated with the average values from the fit of each microring (n = 8-12).

Table S 3.1RMSD of FX Gla-domain mutants from FX-WT in solution

	Protein	Replica 1	Replica 2	Replica 3	Average of all three replicas
	FX-wt	0.88 ± 0.11	0.87 ± 0.12	0.85 ± 0.13	0.86 ± 0.12
Negatively charged residues	γ7D	0.95 ± 0.12	2.26 ± 1.16	1.43 ± 0.28	1.55 ± 0.88
	γ14D	1.59 ± 0.41	1.44 ± 0.20	1.53 ± 0.50	1.52 ± 0.40
	γ19D	0.69 ± 0.11	1.59 ± 0.25	1.70 ± 1.20	1.33 ± 0.84
	γ20D	3.73 ± 0.65	3.60 ± 0.72	1.65 ± 0.19	3.00 ± 1.11
	γ25D	0.92 ± 0.14	3.32 ± 0.98	2.55 ± 0.60	2.26 ± 1.20
	γ29D	1.23 ± 0.26	1.17 ± 0.17	2.10 ± 0.30	1.50 ± 0.49
	γ32D	0.68 ± 0.11	4.86 ± 0.83	7.15 ± 1.56	4.23 ± 2.87
	γ32A	1.46 ± 0.32	1.17 ± 0.21	1.14 ± 0.17	1.25 ± 0.28
Positively charged residues	K9Q	1.11 ± 0.13	1.06 ± 0.20	1.16 ± 0.17	1.11 ± 0.18
	R15Q	1.14 ± 0.17	1.21 ± 0.21	1.13 ± 0.14	1.16 ± 0.18
	R28Q	2.37 ± 0.44	1.12 ± 0.16	1.23 ± 0.20	1.57 ± 0.63

All the mutants were equilibrated for 250 ns with three independent replicas. The RMSD calculation was performed on the last 200 ns of MD simulation.

Table S 3.2 Binding affinities (K_d in μM) of FX-WT and FX Gla-domain mutants

	Protein	50% PS 50% PC
	FX-WT	0.46 ± 0.03
Negatively charged residues	γ7D	NA‡
	γ14D	0.2 ± 0.1
	γ19D	2.9 ± 0.4
	γ20D	NA‡
	γ25D	NA‡
	γ29D	NA‡
	γ32D	0.15 ± 0.06
	γ32A	NA‡
Positively charged residues	K9Q	0.74 ± 0.08
	K10Q	0.5 ± 0.1
	R15Q	2.0 ± 0.3
	R28Q	0.28 ± 0.04

NA‡, No saturable binding for the FX Gla-domain mutants were observed.
Data are mean ± standard error N=3

3.7 Contributions

The binding studies carried out in this study were performed by Dr. Sara Medfisch in high throughput micro-ring resonator in Prof. Ryan Bailey's laboratory in the department of Chemistry at University of Michigan-Ann Arbor. The MD simulation studies of FX Gla-domain mutants were set up by Melanie Muller, M.D. Ph.D. candidate and extended and analyzed by Muyun Lihan, Ph.D. candidate in Prof. Emad Tajkhorshid's laboratory at the Beckman Institute of University of Illinois-Urbana Champaign.

Chapter 4 Elucidating Molecular Interactions Between Blood Coagulation Factor X and Russell's Viper Venom

4.1 Introduction

Envenomation from Russell's Viper, *Daboia russelli* induces severe coagulopathies in the victims ultimately causing death and disability. 5.4 million victims of snakebites have been reported globally,[141] among which 70% of the cases occur in tropical regions of Asian countries[142] where Russell's Viper is considered to be one of the deadliest snakes. The venom from the Russell's viper exhibits hemotoxic properties. It contains an activator of the blood clotting factor X (FX) known as RVV-X which mimics the physiological FX activator of tissue factor and factor VIIa (TF/FVIIa complex) by cleaving the same Arg^{52}- Ile^{53} bond in FX to release the activation peptide and generate FXa. Downstream of the clotting cascade this FXa that forms the prothrombinase complex with activated factor V (FVa) to convert prothrombin to thrombin to generate fibrin clot. The difference in FX activation by RVV-X as compared to the TF/FVIIa complex is that the former does not require negatively charged membrane phospholipids as a catalyst and is more procoagulant in solution,[30, 97] thereby causing thrombotic complications in the victims. However, this potent nature of RVV-X has been utilized as a styptic agent to treat minor cuts and in coagulation research and diagnostic purposes.[143, 144]

Structurally, RVV-X is a metalloproteinase enzyme which consists of a heavy chain of 59KDa and two light chains of 18 and 21 kDa.[145] The two light chains are closely related to various snake venom C-type lectin related proteins also known as Snacles. Previous structural studies showed that the light chain of a homologous snake venom from *Deinagkistrodon acutus* interacted with the FX Gla-domain.[72] The N-terminus of FX contains the γ-carboxyglutamate-rich domain (Gla domain) which adopts a proper conformation in presence of Ca^{2+} ions and engages with membrane phospholipids. Studies have shown that the protein-membrane interactions of FX Gla-domain increased the rates of FX activation by TF/FVIIa complex by thousand-fold,[30] thereby indicating the crucial nature of the molecular interactions mediated by FX Gla-domain in the clotting cascade.

Removal of properly folded FX Gla-domain reduced the affinity of RVV-X for FX by approximately 100-fold.[97] Takeda et al., solved the crystal structure of RVV-X (PDB: 2E3X)[99] and docked FXa to propose the possible interactions between FX and the RVV-X. In agreement with all the previous studies, they proposed that the light chain of RVV-X binds to FX Gla-domain, which prevents the protein-membrane interaction and positions FX properly for activation.

Although these studies have shown that FX Gla-domain engages with RVV-X, the molecular interactions are still unknown. Here, we performed structural alignment studies *in silico* to predict possible FX Gla-domain residues that interact with RVV-X and mutated them to test their effect on the rates of FX activation by RVV-X and further downstream of the clotting cascade to fully understand the implications.

4.2 Materials

Materials used in this study are as follows: Human FX, FVa, prothrombin (PT) and snake venom protease (RVV-X) were from Haematologic Technologies (Essex Junction, VT); methoxycarbonyl-D-Nle-Gly-Arg-pNA acetate salt (FXa substrate) and (Sar-Pro-Arg-pNA) thrombin substrate from Bachem (Bubendorf, Switzerland); medium binding microplate from Corning® (Corning, NY). PureYield™ Plasmid Midiprep System from Promega (Madison,WI); Lipofectamine 2000 and Opti-Mem™ reduced serum media from Thermo Fischer (Waltham,MA); 500 mL DMEM (Dulbecco's Modified Eagle's Medium)/Hams F-12 50/50 Mix from Corning® (Corning, NY);

4.3 Methods

In silico prediction of FX Gla-domain residues in Pymol

Structural alignment of RVV-X with the FX binding protein (XCP) from the snake venom of *Deinagkistrodon acutus (PDB ID: 1IOD)*[72] was carried out by superimposing the crystal structure of RVV-X (PDB ID: 2E3X)[99] on to FX Gla-domain bound to XCP in Pymol 2.5.2. The residues in the snake venom of *Deinagkistrodon acutus* that formed hydrogen or hydrophobic bonds (3.0 – 4.0 Å) with FX Gla-domain and were predicted to interact with RVV-X. These residues were chosen for further mutagenesis studies.

Generation of recombinant FX Gla-domain mutants

FX-WT encoded in pcDNA3.1(+) expression vector from Genscript Biotech (Piscataway,NJ) was used as a template to generate 14 FX Gla-domain mutants: Phe-4 (F4A), Leu-5 (L5A), Gla-7 (γ7D), Lys-9 (K9Q), Lys-10 (K10Q), Gla-25 (γ25D), Arg-28 (R28Q) and Gla-32 (γ32D), (γ32A) by site-directed mutagenesis. 0.5 µg of each plasmid was transfected with Lipofectamine 2000 in HEK293/VKOR cells (HEK 293 cells that overexpress vitamin K 2,3-epoxide reductase C1 expression vector, a kind gift from Darrell Stafford). Transfected HEK293/VKOR cells were selected against 600µg/ml G418 by Fischer scientific (Waltham,MA) and monoclonal stable cell lines were generated by serial dilution method. Expression of FX Gla-domain mutants were carried out in cell factories (Corning HYPER*flask* M Cell Culture Vessel) in DMEM media supplemented with L-glutamine, 15 mM HEPES, 10 µg/ml vitamin K1, 2 µg/ml of puromycin and 400µg/ml of G-418. Expression of recombinant FX Gla-domain mutants were confirmed by FX-Enzyme Linked Immunosorbent Assay (ELISA), Enzyme research laboratory (South Bend, IN). Recombinant FX Gla-domain mutants with HPC4 tag were purified by affinity chromatography as described previously.[123] Subsequently, fully carboxylated FX Gla-domain mutants were purified by anion exchange chromatography column in AKTA Pure (Cytiva, Marlborough,MA).

FX activation assay by RVV-X in solution

18 pM RVV-X, 0.5 mM Spec Xa and 5mM Ca^{2+} was mixed in HBSA (20 mM HEPES, 100mM NaCl, 0.1% BSA). The reaction of FX activation by RVV-X was initiated by adding 0.2 µM FX-WT and FX Gla-domain mutants. The change in the rate was measured spectrophotometrically (milli-OD/min) at A_{405} in Spectramax-96 from Molecular Devices (San Jose,CA).

Prothrombinase assay

Thrombin generation was measured by two-stage discontinuous assay. In the first stage, 100 nM FX-WT and recombinant FX Gla-domain mutants were activated by 1nM RVV-X in 5 mM Ca^{2+} in HBSA. The reaction was quenched after 30 mins with 10 mM EDTA. 0.5 mM Spec Xa was added to 10µl aliquot from the first stage reaction mixture to quantify the amount of FXa generated by referencing to FXa standard curve. In the second stage, activation of prothrombin was carried out as described previously[146], using 450 pM FVa, 330 pM FXa, 400 nM prothrombin, 16.7 µM lipids, 0.5mM substrate in 5 mM Ca^{2+} and HBSA.

4.4 Results

In silico prediction of FX Gla-domain residues interacting with RVV-X

To identify the residues in RVV-X that might interact with FX Gla-domain, we utilized previously published crystal structure of RVV-X (PDB ID:2E3X) and the crystal structure of FX Gla-domain bound to the light chains of snake venom from *Deinagkistrodon acutus* (PDB ID:1IOD). This light chain from the snake venom is also known as the FX binding protein and has been abbreviated as XCP by Mizuno et al.[72] The rationale behind this was to observe the similarity in the tertiary structure of the RVV-X and XCP since they both interact with FX Gla-domain as shown demonstrated previously by various research groups.[72, 97, 99] We hypothesized that the residues in FX Gla-domain that interacted with XCP, would also engage in molecular interactions with RVV-X.

Figure 4.1A shows the structural alignment of the two light chains from RVV-X *(purple)* and XCP *(light pink)* protein. We observed conservation in their tertiary structure. Next, we identified the amino acid residues in FX Gla-domain at positions 4, 5, 7, 9, 10, 25, 28, 29 and 32 that formed interatomic polar or hydrophobic contacts with amino acid residues at position 98, 100, 261, 300, 303, 309 and 312 in the two light chains of XCP (PDB ID:1IOD) in PyMOL 2.5.2. also highlighted with red arrows in Figure 4.1(B & C). Additional details of these interactions are listed in

Table S 4.1, and the molecular interactions are represented in Figure S 4.1. Sequence alignment of the light chains of RVV-X and XCP shown in Figure 4.1B established that they were 48% identical with amino acid residues at position 98 and 261 being fully conserved highlighted *(in yellow)* and *(in blue)* are the conserved amino acid residues at positions 100, 300, 303, 309 and 312, with similar properties. The FX Gla-domain residues interacted with amino acid residues at positions 98, 100, 261, 300, 303. Due to these similarities observed in our *in-silico* studies we chose to mutate the FX Gla-domain residues that interacted with XCP and test their influence on the rates of FX activation by RVV-X in solution. The crystal structure of FX Gla-domain was obtained from the species *Bos Taurus* in PDB ID: 1IOD where the Gln-10 is replaced by a lysine residue in

human FX therefore here we have shown the effects of Lys mutation in position 10. These mutagenesis study would help us to demystify the molecular interactions between FX and RVV-X.

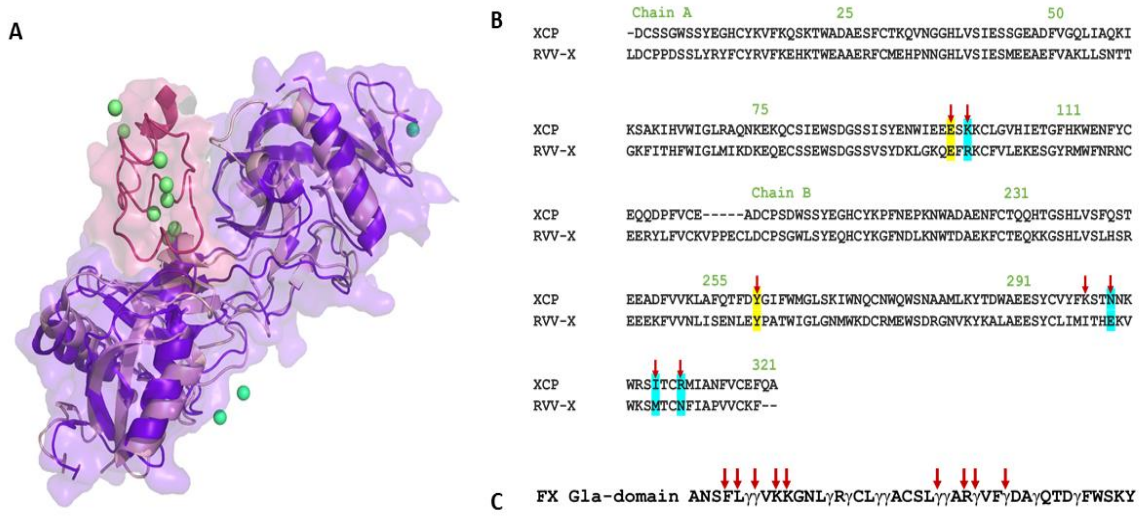

Figure 4.1 **Predicting the FX Gla-domain residues interacting with RVV-X** (A) Represents the structural alignment of the two light chains, Chain A and Chain B *(purple)* of RVV-X PDB ID: 2E3X, on top of the light chain *(light pink)* also known as FX binding protein or XCP is from the snake venom of *Deinagkistrodon acutus* bound to bovine FX Gla-domain *(dark pink)* PDB ID: 1IOD. Calcium ions bound to both the crystal structures are represented as spheres *(green)*. (B) Sequence alignment of XCP and RVV-X the amino acid residue numbers *(green)* of XCP (C) Sequence of human FX Gla-domain and the Gla residues are denoted as γ. Arrows *(red)* represent the residues in light chain of XCP and FX Gla-domain that form interatomic polar or hydrophobic contact in PDB ID: 1IOD. Residues highlighted in *(yellow)* represent the fully conserved residues between XCP and RVV-X and residues highlighted in *(blue)* represent the residues conserved with similar properties.

Impact of mutagenesis on rates of FX activation by RVV-X

We utilized site directed mutagenesis studies to generate the following point mutations Phe-4 (F4A), Leu-5 (L5A), Gla-7 (γ7D), Lys-9 (K9Q), Lys-10 (K10Q), Gla-25 (γ25D), Gla-29 (γ29D), Gla-32 (γ32D and γ32A). To test our hypothesis, we studied the effect of these mutations on the rates of FX activation by RVV-X in solution. The first two mutants F4A and L5A are present in the ω-loop of FX Gla-domain, and they are known to interact with hydrophobic chains of the membrane phospholipids that allows FX to tether to the membrane.[96] In the crystal structure PDB ID: 1IOD, F4 forms both hydrophobic and polar contact with R312 in chain B of XCP whereas the L5 residues engages only in polar contact via the amide bond between F4 and L5 Figure S

4.1A. This correlates well with the mutagenesis of these two residues, where we observed a 40% decrease for F4 but no change in the rates of FX activation by RVV-X for L5 as shown in Figure 4.2. γ7 participated in a hydrophobic interaction with I309 Figure S 4.1B, and mutating γ7D we observed a 90% decrease in the rates of FX activation by RVV-X. The two Lys residues at position 9 and 10 in the FX Gla-domain showed 20-40% reduction in FX activation respectively Figure 4.2B. Mutagenesis of K10 had a greater effect than K9 because it is involved in multiple hydrophobic contacts with the Y261 whereas for K9 we observed only one hydrophobic bond between Y261 of XCP and the carboxylic group of K9 forming the amide bond with K10 Figure S 4.1C. One of the carboxylate group in γ25 made both polar and hydrophobic contacts with K100 of XCP Figure S 4.1D while the other carboxylate group engaged with the Ca^{2+} ion. Mutating γ25D leaves a single carboxylate group which can now only engage either with the Ca^{2+} ion or the K100. Possibly, due to this we observed 80% decrease in the rates of FX activation. Lastly, the carboxylate group in γ32 forms a polar contact with N303 of XCP Figure S 4.1E and mutating γ32D shows negligible effect whereas removing both the carboxylate group in γ32A decreases the rate of FX activation by RVV-X approximately by 30% as shown in Figure 4.2B which suggests that even with one carboxylate group the interaction between Gla-32 and Asn-300 is possible.

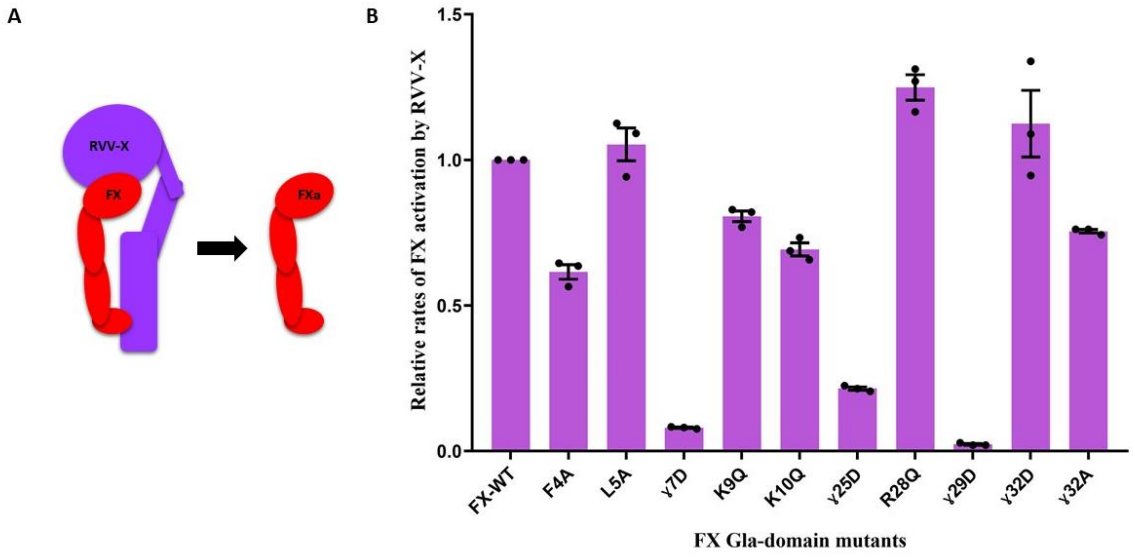

Figure 4.2 **Influence of mutagenesis on the rates of FXa generation by RVV-X**. (A) Cartoon representation of FX *(red)* activation by RVV-X *(purple)* to generate FXa in absence of membrane. (B) The impact of mutating FX Gla-domain residues F4A, L5A, γ7D, K9Q, K10Q, γ25D, R28Q, γ29D, γ32D and γ32A are shown above. The initial rates of FX activation of the FX Gla-domain

mutants were normalized to FX-WT for each day. Data are represented as mean ± standard error N=3.

Influence of mutagenesis of FX Gla-domain mutants on the rates of prothrombin activation

To assess the impact of mutagenesis in the downstream portion of the clotting cascade we further tested the rates of prothrombin activation by FXa containing the Gla-domain mutations. Under normal conditions vascular trauma causes FX activation by the TF/FVIIa complex which initiates the clotting cascade and generates FXa. The FXa generated further forms the prothrombinase complex with FVa and prothrombin (FII) on negatively charged membrane surfaces to generate thrombin as shown in Figure 4.3A. However, envenomation from the Russell's Viper also activates FX and we wanted to study the role of the FX Gla-domain residues Figure 4.3C in thrombin generation that would ultimately affect the clot formation. Research from others have shown that FX Gla-domain does not directly engage with FVa,[47] but participates in protein-membrane interactions. Therefore, we hypothesized that mutagenesis of FX Gla-domain should not have severe impact on thrombin generation. To test our hypothesis, we activated the FX Gla-domain mutants by RVV-X to generate FXa that was further utilized for thrombin generation. We observed that for FX Gla-domain residues F4A, γ7D, γ25D, γ29D, γ32D and γ32A we observed 40-50% reduction in the rates of thrombin generation and for residues L5A, K9Q and K10Q we observed 20-30% reduction as shown in Figure 4.3B. Interestingly, the impact of FX Gla-domain mutagenesis did not have severe impact on the rates of thrombin generation observed in case of FX activation by RVV-X Figure 4.2B or by TF/FVIIa Figure 3.2 (B,C,E & F).

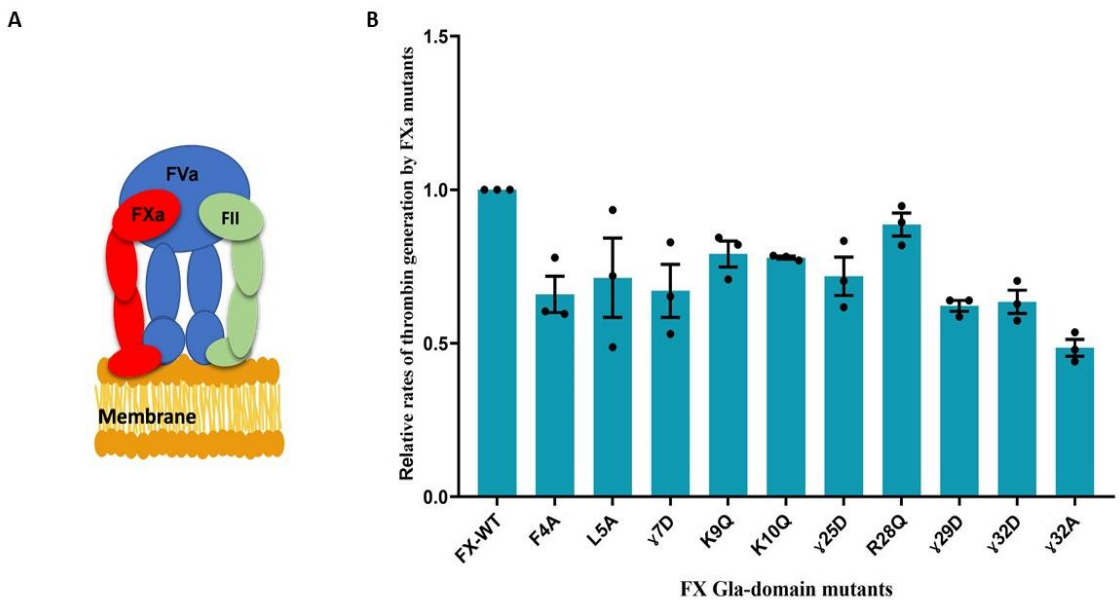

Figure 4.3 **Influence of mutagenesis on the rates of thrombin generation by FXa.** (A) Cartoon representation of thrombin generating complex also known as the Prothrombinase complex. In this study FXa *(red)* was generated by RVV-X which contain the mutated FX Gla-domain. FII *(green)* also known as prothrombin is activated by FXa and FVa *(blue)* on membrane surfaces to form thrombin. (B) The impact of mutating FX Gla-domain residues F4A, L5A, γ7D, K9Q, K10Q, γ14D, R15Q, γ19D, γ20D, γ25D, R28Q, γ29D, γ32D and γ32A on the rates of thrombin generation are shown above. The initial rates of prothrombin activation in presence of FX Gla-domain mutants on 20% POPS and 80% POPC membrane surfaces were normalized to FX-WT for each day. Data are represented as mean ± standard error N=3.

4.5 Discussion

The snake venom protease, RVV-X, possibly recognizes the FX Gla-domain to activate the clotting cascade artificially. Therefore, elucidating the molecular interactions between FX and RVV-X would help understanding the initial steps in FX activation by RVV-X and aid in the development of therapeutic efforts for snakebite victims. Here by utilizing in silico prediction methods we identified key amino acid residues in the FX Gla-domain that formed polar or hydrophobic contacts with RVV-X and further mutated them to study their influence on the rates of FX activation by RVV-X. Mutagenesis of three FX Gla-domain residues γ7, γ25 and γ29 severely impacted the rates of FX activation whereas in case of γ32 we observed that a single carboxylate group was capable of maintaining the intermolecular interactions between FX Gla-domain and RVV-X. In the ω-loop of FX Gla-domain mutagenesis of hydrophobic residue F4 was 40% more detrimental than L5 for rates of FX activation indicating that the phenylalanine ring was

able to form multiple polar and π-π interactions with RVV-X necessary for proper FX activation. Mutagenesis of FX Gla-domain residues at position 9, 10 and 28 did not have drastic effects on rates of FX activation. To further understand the implication of these interactions in downstream clotting cascade, we also tested their impact on thrombin generation. Interestingly, none of the mutants severely impacted thrombin generation since we did not observe greater than 50% reduction for thrombin generation in presence of the activated FX Gla-domain mutants. The mutants that affected severely the rates of FX activation by RVV-X slowly generated FXa which will eventually delay in thrombin generation. Thus, the molecular interactions between RVV-X and FX Gla-domain are the determining factor for clot formation when FX is activated externally. Finally, looking at the FX Gla-domain residues that upon mutagenesis showed 30-90% decrease in the rates of FX activation by RVV-X are clustered together shown in Figure 4.4 which suggests a probable binding interface between FX Gla-domain and RVV-X.

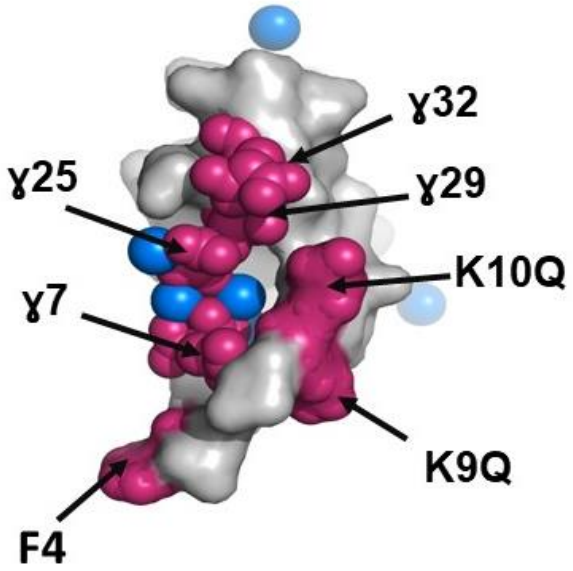

Figure 4.4 **Probable binding interface between FX Gla-domain and RVV-X.** FX Gla-domain is shown as surface representation in *grey*. FX Gla-domain residues that reduced the rates of FX activation by RVV-X by 30-90% as compared to the FX-WT are highlighted here in *dark pink*. The calcium ions bound to the FX Gla-domain are shown in *blue*.

4.6 Supplementary figures and tables

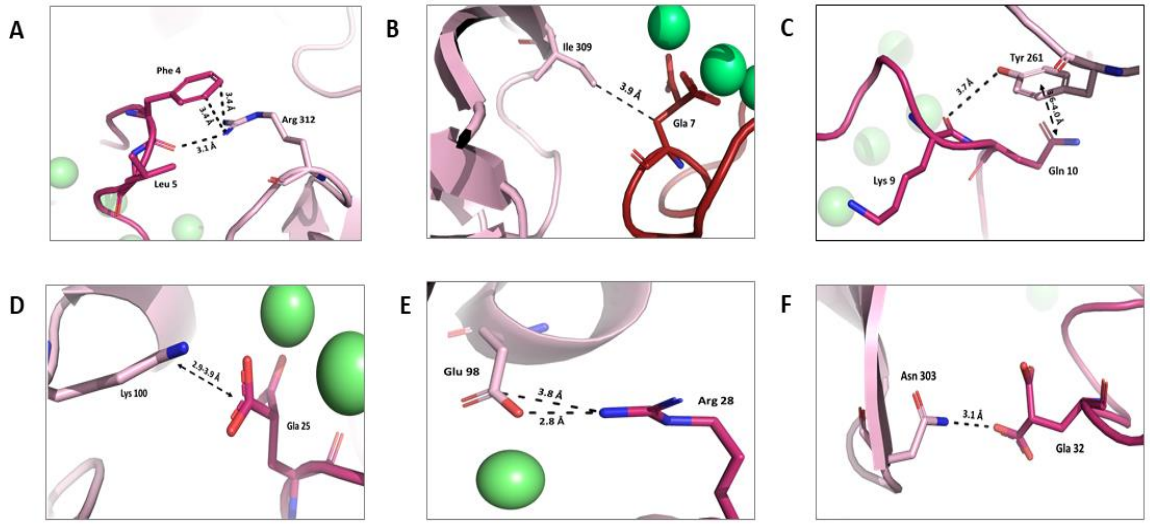

Figure S 4.1 **Intermolecular interactions between FX Gla-domain and XCP:** The intermolecular interactions between the FX Gla-domain *(dark pink)* and the FX binding protein or the XCP in *(light pink)* observed in the crystal structure PDB ID:1IOD[72] are shown here. The amino acid residues involved in the molecular interactions are discussed as follows and the respective protein to which they belong to are denoted as *FX* and *XCP* in the superscript (A) The backbone amide bone of Phe-4^{FX} and Leu-5^{FX} forms a polar contact with XCP residue Arg-312^{XCP}. Phe-4^{FX} also formed additional hydrophobic contacts. (B) Hydrophobic interaction observed between Gla-7^{FX} and Ile-309^{XCP}. (C) Multiple hydrophobic interactions observed between Gln-10^{FX} and Tyr-261^{XCP} and hydrophobic interaction observed between Lys-9^{FX} and Tyr-261^{XCP} (D) The carboxylate group of Gla-25 is forming polar and hydrophobic interactions with Lys-100^{XCP}. (E) Arg-28^{FX} forms both polar and hydrophobic interactions with Glu-98^{XCP}. (F) Carboxylic group of Gla-32^{FX} is interacting with Asn-303^{XCP}.

Table S 4.1 Interactions between FX Gla-domain and residues in FX binding protein from snake venom

FX Gla-domain residues	Residues in XCP	Distance (in Å)	Type of interaction
Phe-4 (F4)	R312_Chain B	3.1	[a]Polar contacts
Leu-5 (L5)	R312_Chain B	3.1	Polar contact
Gla-7 (γ7)	I309_Chain B	3.9	[b]Hydrophobic contact
Lys-9 (K9)	Y261_Chain B	3.7	Hydrophobic contact
Gln-10 (Q10)	Y261_Chain B	3.6-4.0	Hydrophobic contacts
Gla-25 (γ25)	K100_Chain A	2.7-3.7	Polar and hydrophobic contacts
Arg-28 (R28)	E98_Chain A	2.8 & 3.8	Polar and hydrophobic contact
Gla-29 (γ29)	K300_Chain B	2.9-3.9	Polar and hydrophobic contacts
Gla-32 (γ32)	N303_Chain B	3.1	Polar contact

The molecular interactions listed in this table were identified in the crystal structure of FX Gla-domain bound to XCP PDB ID: 1IOD and visualized in PyMOL 2.5.2.
[a]Polar contacts are identified as the distance between the atom centers that are less than 3.5 Å.
[b]Hydrophobic contacts are identified as the distance between the atom centers that are in the range between 3.5 – 4.0 Å.

Chapter 5 Proteins and Ions Compete for Membrane Interaction: the Case of Lactadherin.[c]

5.1 Introduction

Lactadherin, originally identified as a milkfat globule glycoprotein, is known to bind to the plasma membrane via interactions with the anionic lipid phosphatidylserine (PS). Lactadherin has been found to participate in a number of cellular processes including bilayer stabilization, [147] mediating apoptotic clearance of lymphocytes[148, 149] and epithelial cells,[150] and clearing amyloid ß-peptide, a key component of Alzheimer disease. Lactadherin has also been found to help regulate the blood coagulation cascade by acting as an anticoagulant.[151]

Bovine lactadherin, studied here, is comprised of four domains, two epidermal growth factor domains and two discoidin domains (EGF1-EGF2-C1-C2). The C2 domain of lactadherin (LactC2) (Fig. 1) has been found to be the primary location of PS binding.[152]

LactC2 functions as an anticoagulant by blocking PS binding sites from use by coagulation factors such as factor VIII, the prothrombinase complex, and the factor VIIa-tissue factor complex, many of which are mediated by divalent calcium ion (Ca^{2+})-PS interactions. Unlike many of the components of the coagulation cascade, LactC2 does not require Ca^{2+} to mediate interactions with the membrane surface, but still acts as an inhibitor to several clotting proteins. Based on these competitive observations, one possible mechanistic explanation for LactC2's anticoagulant properties are direct competition between LactC2 and Ca^{2+} for PS binding sites. Alternatively, lactadherin's anti-coagulant properties may be derived from its high binding affinity for PS-containing membranes. A previous study of LactC2 binding to PS-containing vesicles, suggests

[c] This chapter has been adapted from a research article published as a preprint in bioRxiv. Full citation: De Lio A.M., Paul D., Jain R., Morrissey J.H. & Pogorelov T.V. (2020) Proteins and ions compete for membrane interaction: the case of Lactadherin. **doi:** 10.1101/2020.04.03.023838

that LactC2's binds just as tightly to the membrane as human factor X, and more tightly than the 6 other human GLA domain-containing clotting proteins on PS-containing nanodiscs.[116, 153]

The LactC2 domain is structurally like the C2 domains in some blood coagulation factors, such as factor V (fV-C2) and factor VIII (fVIII-C2). LactC2, fV-C2, and fVIII-C2 all contain long loops, here referred to as Spikes, that are comprised of water-exposed hydrophobic residues. Site-directed mutagenesis of these hydrophobic residues has highlighted their importance in the functionality of lactadherin. It has been hypothesized that the hydrophobic residues of these Spikes insert into the membrane[154], but detailed studies are lacking. Characterizing the types of interactions that take place at the membrane surface can aid in our understanding of lactadherin's role as a coagulation cascade regulator and, more generally, how charged molecular moieties affect and shape the plasma membrane.

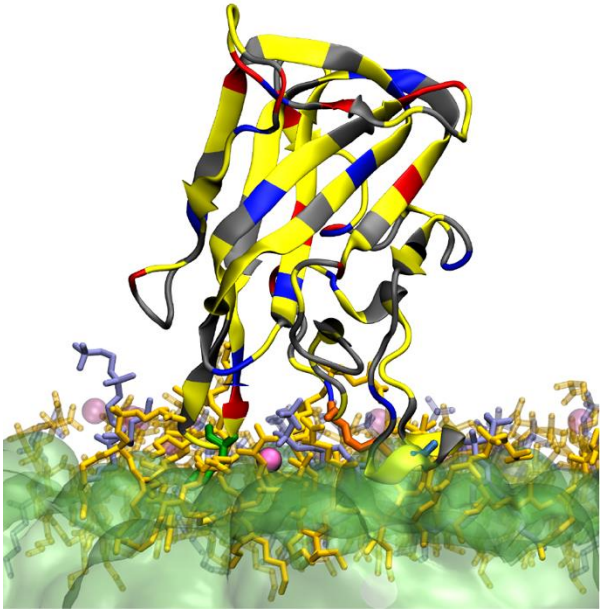

Figure 5.1 **Lact C2 interacting with the membrane.** Snapshot of LactC2 inserted in the short-tail PS in *orange*/PC in *gray-blue* HMMM plasma membrane with dichloroethane (DCLE) in *green* solvent in the presence of Ca2+ in *pink*. Transparent lipids and Ca2+ are farther than 3Å from LactC2 residues. Residues colored by type: polar *gray*, non-polar in *yellow*, basic in *blue*, and acidic in *red*.

Not only do the interactions between the spikes of LactC2 and the membrane affect the coagulation cascade, they also dictate the formation of aortic medial amyloids (AMA), which are present in 97% of the Caucasian population over 50 years of age[155] and may be linked to thoracic aneurysms [156, 157]. Since the peptide forming the AMAs, medin, is derived from the region spanning Spikes 2 & 3 of the human LactC2 domain, characterizing the dynamics and interaction potentials between lactadherin and the plasma membrane are critical for elucidating the biochemical properties of lactadherin.

Here we describe only the experimental nanodisc binding studies conducted in the Morrissey Lab to determine the competitive nature of LactC2-PS and Ca^{2+}-PS interactions. Characterization

of key charged species-lipid interactions both in the presence and absence of Ca^{2+} are also presented.

5.2 Materials

POPC and POPS lipids, purchased from Avanti Polar Lipids (Alabaster, AL), were used to prepare the nanodiscs used in this study. Bio-Beads® SM-2 adsorbent was purchased from Bio-Rad. Bovine Lactadherin was purchased from Hematologic Technologies (Essex Junction, VT). For the Biacore binding studies we purchased the series S Nitrilotriacetic acid Biacore sensor chips from GE Healthcare. The recombinant His-Tagged MSP was expressed in *Escherichia coli* BL21 DE3 cells (Agilent technologies) and purified in AKTA start system (GE Healthcare Life Science) by Ni NTA(Qiagen) column.

5.3 Methods

Preparation of Nanodiscs

Quantification of the binding constants for lactadherin to PS containing membranes were done with nanodiscs. Nanodiscs are soluble monodisperse discoidal lipid/protein particles with controlled size and phospholipid composition where the lipid bilayer is surrounded by a helical protein belt termed as membrane scaffold proteins (MSP).[112] To prepare the nanodiscs, a total of 3.9 μmol of phospholipids comprised of 70% POPS and 30% POPC were prepared in chloroform and dried under compressed nitrogen. Nanodiscs comprised of 100 % PC were also prepared as a negative control for the binding studies. The residual chloroform from the lipids was removed overnight under high vacuum. The lipids were dissolved in a 100 mM sodium deoxycholate, 20mM Tris, and 100mM NaCl buffer solution and incubated with MSP for 2 hrs at 4°C. The detergent was removed post incubation via Bio-Beads at 4°C for 4 hours in a rotator. This allowed the self-assembly of the nanodiscs. The nanodiscs were further purified by size exclusion chromatography (SEC) in Akta Pure with the Superdex 200 10/300 GL column (GE healthcare Life Sciences).

Surface Plasmon Resonance Analysis of Lactadherin binding to Nanoscale Bilayers

The binding affinities for lactadherin to the nanodiscs in the presence and absence of 5 mM Ca^{2+} were quantified by surface plasmon resonance (SPR) on a GE Biacore T-200 instrument. His-

Tagged nanodiscs were loaded on the Ni-NTA surface sensor chip in a solution of 20 mM HEPES and 100 mM NaCl. The flow rate of lactadherin was set to 30 uL/min and the binding was monitored in real time as the concentration of lactadherin was increased from 25 nM to 2.5 μM. The surface equilibration time for the binding studies was 110 seconds. Several concentrations of lactadherin were used to study membrane association (Fig. S8), a representative result for 800 nM lactadherin can be found in Fig. 5B. Experiments were completed in triplicate with fresh samples.

As reported previously (7), the binding isotherms were plotted from maximal steady-state response units versus the protein concentration flowed over the chip surface, from which the equilibrium binding constant, K_d, values were derived by fitting the single-site ligand binding equation to the data in Graph Pad Prism 8.0. The single-site ligand binding equation is:

$$Y = \frac{B_{max} * X}{K_d + X},$$

Specific binding of lactadherin was corrected by normalizing it to the 100% PC nanodiscs. The non-linear curve of the binding data was analyzed by fitting it to the monomolecular growth model equation:

$$y = m_1 - m_2^{m_3 x},$$

as shown previously by Qi et al.[158] We used this equation to calculate the $k_{observed}$ for various LactC2 concentration. The k_{on} was derived from the slope of the $k_{observed}$ versus concentration plot in Fig. S8.

5.4 Results

Binding Studies

Surface plasmon resonance (SPR) studies of lactadherin on PS/PC nanodiscs were performed in order to determine whether the presence of Ca^{2+} moieties affects the binding affinity Figure 5.2A The representative raw sensorgram for lactadherin binding to nanaodiscs at 800nM concentration is shown in Figure 5.2C. To our knowledge, this is the first report on the binding affinity of lactadherin using nanodiscs as the membrane model. We find that the binding affinity in the absence of Ca^{2+} is 296.2 ± 82.8 nM, which is in agreement with previously reported literature.[153] In order to more accurately model a physiologically relevant system, we also

measured the binding affinity of lactadherin in the presence of Ca^{2+}; which was measured to be 283.0 ± 66.5 nM. These values suggest that there is no change in the binding affinity of lactadherin to the membrane model in the presence and absence of Ca^{2+} Figure 5.2A. Since LactC2 binds PS in a Ca^{2+}-independent manner,[151] we expected to observe similar binding affinities in both systems. This is also in agreement with our computational observation that LactC2-PS interactions occur regardless of the presence or absence of Ca^{2+}.[159]

We hypothesized that Ca^{2+} and the charged residues of the Spikes would compete for the charged lipid headgroup binding sites of the membrane. We used SPR to determine if the association time and association rates of lactadherin to the membrane were affected by the presence of Ca^{2+} Figure 5.2B. To estimate the k_{on} shown in Figure S 5.2 values for lactadherin in the presence and absence of Ca^{2+} only the association rates of lactadherin binding to the membrane shown in Figure S 5.1 were utilized. The k_{on} was not significantly different enough to suggest competition between lactadherin and Ca^{2+} Figure S 5.2 and Figure 5.2C, and therefore suggest that lactadherin's anticoagulant properties do not simply stem from this type of competition. Instead, lactadherin's anticoagulant properties could stem from its binding affinity to the membrane. In a 50% PS and 50% PC nanodisc, the K_d of factor X was reported as 380 ± 5 nM.[116]

5.5 Discussion

In conjunction with SPR binding studies, we also captured the spontaneous interaction with and insertion into the lipid bilayer of the LactC2 domain. Our SPR measurements on PS:PC nanodiscs suggest that lactadherin's binding affinity and binding association times to the membrane are unaffected by the presence of Ca^{2+}. All-atom MD simulations[159] corroborate these observations and suggest that spontaneous interaction and insertion of LactC2's Spikes occur both in the presence and absence of Ca^{2+}. These finding suggest that lactadherin's anticoagulant properties are not simply a result of PS site competition with Ca^{2+} but could be related to competition with blood clotting factors for membrane binding sites. This is evidenced by our reported low K_d value both in the presence and absence of Ca^{2+}; suggesting lactadherin has a similar binding affinity to factor X, the blood clotting factor with the tight membrane binding. This study provides new insight into the mechanism that drives the anticoagulant properties of lactadherin and will guide our future studies into determining lactadherin's mechanism of anticoagulation, characterizing the effect the charged residues on Spikes 1-3 have on the shape and

functionalization of the lipids in the membrane, and determining the functionality of the LactC2-derived medin amyloid fibrils.

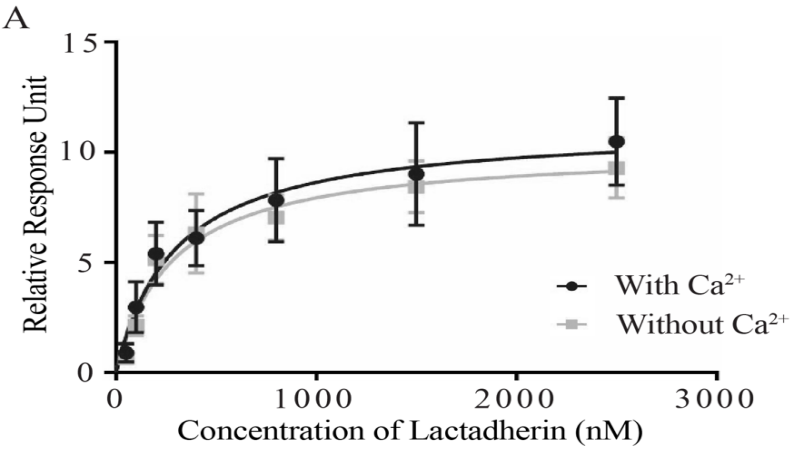

C

	Binding Affinity K_d (nM)	Association Rate k_{on} ($M^{-1}s^{-1}$)
With Ca^{2+}	296.2 ± 82.8	$5.2x10^{-5}$
Without Ca^{2+}	283.0 ± 66.5	$4.1x10^{-5}$

Figure 5.2 **Experimental studies on lactadherin binding to PC/PS nanodiscs.** (A) Comparison of binding affinities of lactadherin to nanodiscs containing 70% PS and 30% PC in the presence (*black*) and absence of (*gray*) Ca^{2+} at multiple lactadherin concentrations. (B) Association times of lactadherin in the presence of (black) and absence of (*gray*) Ca^{2+} with a lactadherin concentration of 800 nM. (C) Binding affinities and association rates for both systems. The k_{on} was calculated using all the concentrations shown in Figure S 5.2 **. Comparison of association rates (kon) of lactadherin to the nanodiscs**. The slope of rate versus concentration lines approximate the kon values were estimated in the absence of Ca2+ (red) and in the presence of Ca2+ (blue).

5.6 Supplementary figures

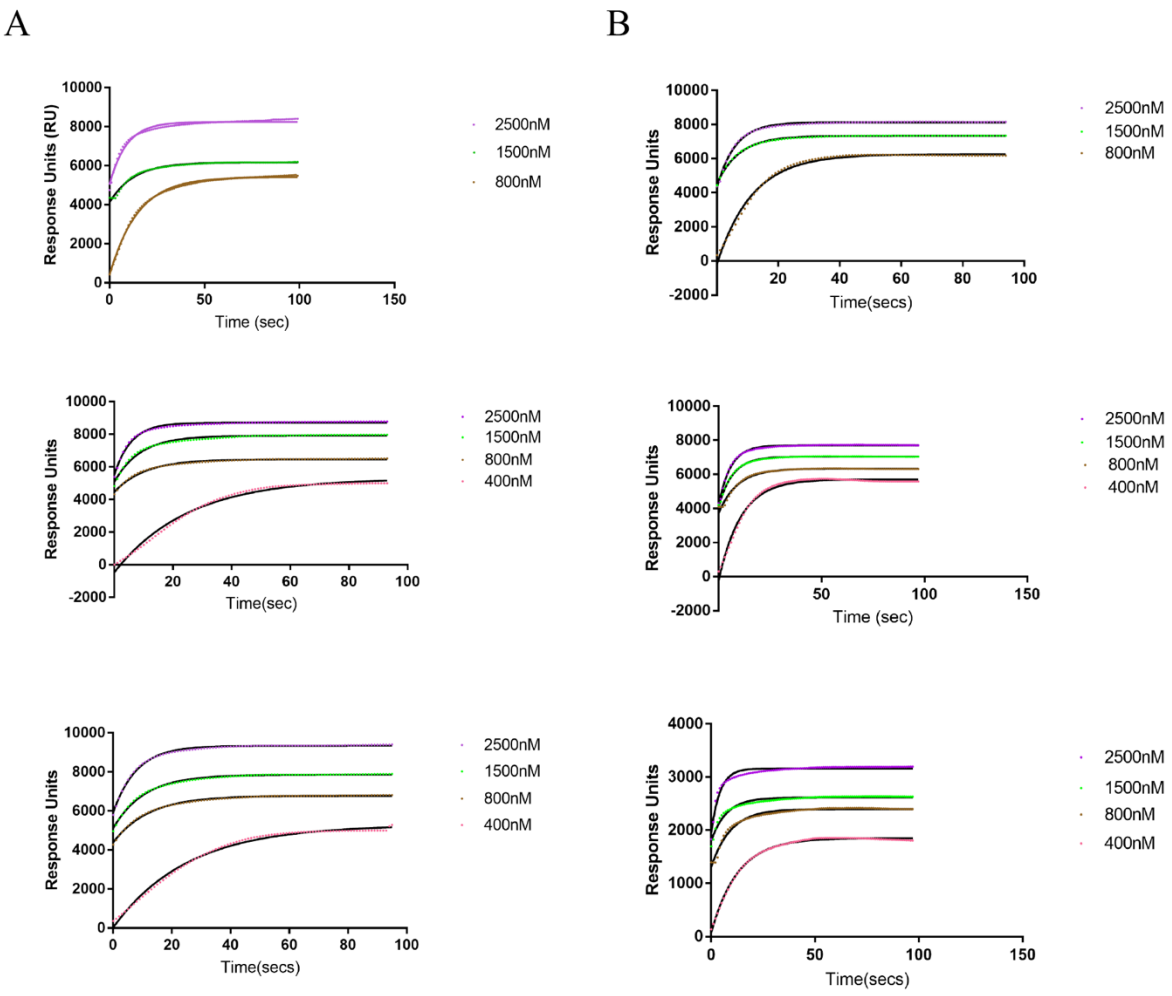

Figure S 5.1 **Raw data showing the association of lactadherin to nanodiscs**. Both with (A) and without (B) Ca^{2+} and each experiment was completed in triplicate the results from each individual experiment are shown.

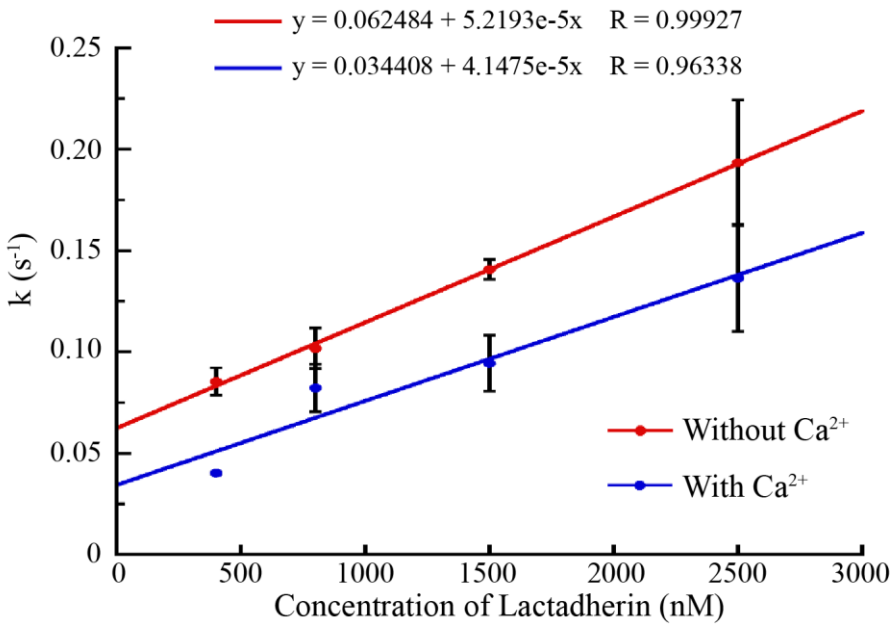

Figure S 5.2 **. Comparison of association rates (k_{on}) of lactadherin to the nanodiscs.** The slope of rate versus concentration lines approximate the k_{on} values were estimated in the absence of Ca^{2+} (red) and in the presence of Ca^{2+} (blue).

Conclusion

An important step in the initiation of the clotting cascade is soluble FX binding to anionic membrane phospholipids such as PS. Previous studies have shown that a single binding site for FX consists of 6-8 PS molecules[128], but these estimates were made with membranes containing high PS concentrations (in binary mixtures of PS and PC) that do not occur in physiology. Since PE is more abundant than PS and studies have shown it synergizes with PS to enhance the rates of FX activation by TF/FVIIa complex,[94] we revisited the phospholipid composition of a single binding site for FX in membranes containing PS and PE. Binding studies carried out in Chapter 2 showed that FX requires a single PS molecule to bind membranes containing excess PE[139]. Thus, we can imagine that a single FX binding site possibly, consists of 6-8 phospholipids comprising of at least one PS and other PE molecules. Since one PS molecule is necessary for FX binding to the membranes, it suggests that there might a unique PS binding site in the Gla-domain of FX. Tavoosi et al., showed that FX Gla-domain binds L-PS with three times tighter binding affinity as compared to D-PS,[116] which suggests that FX Gla-domain recognizes the chiral center in the amino functional group of the PS headgroup. The PE headgroup lacks this chiral center and as per the ABC (Anything But Choline) hypothesis,[94] the phosphate functional group of PE interacts with FX Gla-domain to support the binding. Therefore, in Chapter 3 we further investigated the roles of the amino and phosphate functional groups of the PS headgroup in the protein-membrane interaction of the FX Gla-domain at the molecular level. We tested the influence of mutating the amino acid residues in FX Gla-domain that were predicted to interact with the two functional groups of the PS headgroup, on membrane binding and FX activation rates by TF/FVIIa complex. Our studies showed that the FX Gla-domain amino acid residues that were predicted in MD studies to interact with the amino functional group of the PS headgroup were crucial for membrane binding.

Hence, these studies support the idea of a unique PS binding site in the FX Gla-domain that cannot be replaced by PE. One possible scenario could be a binding pocket that would allow the L-PS headgroup to dock and this binding site is most likely to be lined with Gla residues. To answer these questions, further structural studies such as observing NMR chemical shifts upon PS binding

of isotopically labeled FX Gla-domain can provide the blueprint of this PS binding site. Since FX remains an attractive drug target because of its central position in the clotting cascade, identifying this binding site can potentially allow development of therapies for regulating the clotting cascade in a specific manner unlike the current FXa DOACs (Direct Oral Anticoagulants) which carry a risk of bleeding in patients[160].

Mutagenesis studies revealed that mutating Gla-7, Gla-20 or Gla-29 in FX Gla-domain were highly detrimental to membrane binding of FX and these mutations also impacted FX activation rates by TF/FVIIa complex. In Chapter 4 we observed that mutating these Gla residues also diminished FX activation by an external FX activator from Russel's Viper Venom known as RVV-X. Previous biochemical studies showed that in absence of Gla-domain, FX served as a poor substrate for RVV-X. Therefore, it was hypothesized that to trigger the blood clotting cascade artificially, RVV-X prevents the membrane binding of FX by directly interacting with the Gla-domain. In our study we found a probable binding interface containing Gla-7, Gla-20 and Gla-29 in the FX Gla-domain which might face towards the RVV-X for establishing suitable molecular interactions. A more direct approach of observing these interactions would be to solve the crystal structure of RVV-X bound to the FX Gla-domain. Additionally, we found that the anticoagulant properties of lactadherin, might be due to the direct competition between clotting proteins such as FX to bind PS and not with Ca^{2+} ions as observed in Chapter 5.

In conclusion, this study paves the way for designing therapeutics for targeting the membrane binding of FX in the clotting cascade to regulate the thrombin generation. Further, we have expanded the understanding of the role of FX Gla-domain residues in the membrane binding which can perhaps be utilized in future for developing a recombinant FX therapy for treating pathological conditions such as thrombosis. Lastly, current treatments for treating the victims of snake bites are non-specific. Peptides designed against the FX binding site for RVV-X to disrupt the molecular interactions between the two molecules could perhaps be utilized for treating snakebite victims.

Bibliography

[1] Bhagavan, N. V. (2002) CHAPTER 36 - Biochemistry of Hemostasis, In *Medical Biochemistry (Fourth Edition)* (Bhagavan, N. V., Ed.), pp 839-872i, Academic Press, San Diego.

[2] Neuenschwander, P. F., Branam, D. E., and Morrissey, J. H. (1993) Importance of substrate composition, pH and other variables on tissue factor enhancement of factor VIIa activity, *Thrombosis and Haemostasis 70*, 970-977.

[3] Lawson, J. H., Butenas, S., and Mann, K. G. (1992) The evaluation of complex-dependent alterations in human factor VIIa, *Journal of Biological Chemistry 267*, 4834-4843.

[4] Zwaal, R. F., Comfurius, P., and Bevers, E. M. (1998) Lipid-protein interactions in blood coagulation, *Biochimica et Biophysica Acta 1376*, 433-453.

[5] Tavoosi, N., Smith, S. A., Davis-Harrison, R. L., and Morrissey, J. H. (2013) Factor VII and protein C are phosphatidic acid-binding proteins, *Biochemistry 52*, 5545-5552.

[6] Hertzberg, M. (1994) Biochemistry of factor X, *Blood Reviews 8*, 56-62.

[7] Rosenberg, R. D., and Bauer, K. A. (1987) Thrombosis in inherited deficiencies of antithrombin, protein C, and protein S, *Human Pathology 18*, 253-262.

[8] Scambler, P. J., and Williamson, R. (1985) The structural gene for human coagulation factor X is located on chromosome 13q34, *Cytogenetics and Cell Genetics 39*, 231-233.

[9] Presnell, S. R., and Stafford, D. W. (2002) The vitamin K-dependent carboxylase, *Thrombosis and Haemostasis 87*, 937-946.

[10] Hansson, K., and Stenflo, J. (2005) Post-translational modifications in proteins involved in blood coagulation, *Journal of Thrombosis and Haemostasis : JTH 3*, 2633-2648.

[11] Rezaie, A. R., Neuenschwander, P. F., Morrissey, J. H., and Esmon, C. T. (1993) Analysis of the functions of the first epidermal growth factor-like domain of factor X, *Journal of Biological Chemistry 268*, 8176-8180.

[12] Venkateswarlu, D., Perera, L., Darden, T., and Pedersen, L. G. (2002) Structure and dynamics of zymogen human blood coagulation factor X, *Biophys Journal 82*, 1190-1206.

[13] Fujikawa, K., Legaz, M. E., and Davie, E. W. (1972) Bovine factors X 1 and X 2 (Stuart factor). Isolation and characterization, *Biochemistry 11*, 4882-4891.

[14] Bajaj, S. P., Rapaport, S. I., and Brown, S. F. (1981) Isolation and characterization of human factor VII. Activation of factor VII by factor Xa, *Journal of Biological Chemistry 256*, 253-259.

[15] Radcliffe, R., and Nemerson, Y. (1975) Activation and control of factor VII by activated factor X and thrombin. Isolation and characterization of a single chain form of factor VII, *Journal of Biological Chemistry 250*, 388-395.

[16] Muller, Y. A., Ultsch, M. H., and de Vos, A. M. (1996) The Crystal Structure of the Extracellular Domain of Human Tissue Factor Refined to 1.7 Å Resolution, *Journal of Molecular Biology 256*, 144-159.

[17] Ruf, W., Rehemtulla, A., Morrissey, J. H., and Edgington, T. S. (1991) Phospholipid-independent and -dependent interactions required for tissue factor receptor and cofactor function, *Journal of Biological Chemistry 266*, 2158-2166.

[18] Norledge, B. V., Petrovan, R. J., Ruf, W., and Olson, A. J. (2003) The tissue factor/factor VIIa/factor Xa complex: a model built by docking and site-directed mutagenesis, *Proteins 53*, 640-648.

[19] Venkateswarlu, D., Duke, R. E., Perera, L., Darden, T. A., and Pedersen, L. G. (2003) An all-atom solution-equilibrated model for human extrinsic blood coagulation complex (sTF-VIIa-Xa): a protein-protein docking and molecular dynamics refinement study, *Journal of Thrombosis and Haemostasis : JTH 1*, 2577-2588.

[20] Lee, C. J., Chandrasekaran, V., Wu, S., Duke, R. E., and Pedersen, L. G. (2010) Recent estimates of the structure of the factor VIIa (FVIIa)/tissue factor (TF) and factor Xa (FXa) ternary complex, *Thrombosis Research 125 Suppl 1*, S7-s10.

[21] Ruf, W., Miles, D. J., Rehemtulla, A., and Edgington, T. S. (1992) Tissue factor residues 157-167 are required for efficient proteolytic activation of factor X and factor VII, *Journal of Biological Chemistry 267*, 22206-22210.

[22] Carlsson, K., Freskgård, P. O., Persson, E., Carlsson, U., and Svensson, M. (2003) Probing the interface between factor Xa and tissue factor in the quaternary complex tissue factor-factor VIIa-factor Xa-tissue factor pathway inhibitor, *European Journal of Biochemistry 270*, 2576-2582.

[23] Roy, S., Hass, P. E., Bourell, J. H., Henzel, W. J., and Vehar, G. A. (1991) Lysine residues 165 and 166 are essential for the cofactor function of tissue factor, *Journal of Biological Chemistry 266*, 22063-22066.

[24] Huang, Q., Neuenschwander, P. F., Rezaie, A. R., and Morrissey, J. H. (1996) Substrate recognition by tissue factor-factor VIIa. Evidence for interaction of residues Lys165 and Lys166 of tissue factor with the 4-carboxyglutamate-rich domain of factor X, *Journal of Biological Chemistry 271*, 21752-21757.

[25] Manithody, C., Yang, L., and Rezaie, A. R. (2007) Identification of a Basic Region on Tissue Factor that Interacts with the First Epidermal Growth Factor-like Domain of Factor X, *Biochemistry 46*, 3193-3199.

[26] Thiec, F., Cherel, G., and Christophe, O. D. (2003) Role of the Gla and first epidermal growth factor-like domains of factor X in the prothrombinase and tissue factor-factor VIIa complexes, *Journal of Biological Chemistry 278*, 10393-10399.

[27] Ndonwi, M., Broze, G., Jr., and Bajaj, S. P. (2005) The first epidermal growth factor-like domains of factor Xa and factor IXa are important for the activation of the factor VII--tissue factor complex, *Journal of Thrombosis and Haemostasis : JTH 3*, 112-118.

[28] Zhong, D., Bajaj, M. S., Schmidt, A. E., and Bajaj, S. P. (2002) The N-terminal epidermal growth factor-like domain in factor IX and factor X represents an important recognition motif for binding to tissue factor, *Journal of Biological Chemistry 277*, 3622-3631.

[29] Ndonwi, M., Broze, G. J., Jr., Agah, S., Schmidt, A. E., and Bajaj, S. P. (2007) Substitution of the Gla domain in factor X with that of protein C impairs its interaction with factor VIIa/tissue

factor: lack of comparable effect by similar substitution in factor IX, *Journal of Biological Chemistry 282*, 15632-15644.

[30] Neuenschwander, P. F., and Morrissey, J. H. (1994) Roles of the membrane-interactive regions of factor VIIa and tissue factor. The factor VIIa Gla domain is dispensable for binding to tissue factor but important for activation of factor X, *Journal of Biological Chemistry 269*, 8007-8013.

[31] Ruf, W., Shobe, J., Rao, S. M., Dickinson, C. D., Olson, A., and Edgington, T. S. (1999) Importance of factor VIIa Gla-domain residue Arg-36 for recognition of the macromolecular substrate factor X Gla-domain, *Biochemistry 38*, 1957-1966.

[32] Klingler, O., Matter, H., Schudok, M., Bajaj, S. P., Czech, J., Lorenz, M., Nestler, H. P., Schreuder, H., and Wildgoose, P. (2003) Design, synthesis, and structure-activity relationship of a new class of amidinophenylurea-based factor VIIa inhibitors, *Bioorganic & Medicinal Chemistry Letters 13*, 1463-1467.

[33] Vadivel, K., and Bajaj, S. P. (2012) Structural biology of factor VIIa/tissue factor initiated coagulation, *Frontiers in Bioscience (Landmark edition) 17*, 2476-2494.

[34] Ruf, W. (1994) Factor VIIa residue Arg290 is required for efficient activation of the macromolecular substrate factor X, *Biochemistry 33*, 11631-11636.

[35] Mazurkiewicz-Pisarek, A., Płucienniczak, G., Ciach, T., and Płucienniczak, A. (2016) The factor VIII protein and its function, *Acta Biochimica Polonica 63*, 11-16.

[36] van Dieijen, G., Tans, G., Rosing, J., and Hemker, H. C. (1981) The role of phospholipid and factor VIIIa in the activation of bovine factor X, *Journal of Biological Chemistry 256*, 3433-3442.

[37] Lapan, K. A., and Fay, P. J. (1997) Localization of a factor X interactive site in the A1 subunit of factor VIIIa, *Journal of Biological Chemistry 272*, 2082-2088.

[38] Lapan, K. A., and Fay, P. J. (1998) Interaction of the A1 subunit of factor VIIIa and the serine protease domain of factor X identified by zero-length cross-linking, *Thrombosis and Haemostasis 80*, 418-422.

[39] Celie, P. H., Lenting, P. J., and Mertens, K. (2000) Hydrophobic contact between the two epidermal growth factor-like domains of blood coagulation factor IX contributes to enzymatic activity, *Journal of Biological Chemistry 275*, 229-234.

[40] Chang, Y. J., Wu, H. L., Hamaguchi, N., Hsu, Y. C., and Lin, S. W. (2002) Identification of functionally important residues of the epidermal growth factor-2 domain of factor IX by alanine-scanning mutagenesis. Residues Asn(89)-Gly(93) are critical for binding factor VIIIa, *Journal of Biological Chemistry 277*, 25393-25399.

[41] Rezaie, A. R. (2000) Identification of basic residues in the heparin-binding exosite of factor Xa critical for heparin and factor Va binding, *Journal of Biological Chemistry 275*, 3320-3327.

[42] Rudolph, A. E., Porche-Sorbet, R., and Miletich, J. P. (2000) Substitution of asparagine for arginine 347 of recombinant factor Xa markedly reduces factor Va binding, *Biochemistry 39*, 2861-2867.

[43] Rudolph, A. E., Porche-Sorbet, R., and Miletich, J. P. (2001) Definition of a factor Va binding site in factor Xa, *Journal of Biological Chemistry 276*, 5123-5128.

[44] Heeb, M. J., Kojima, Y., Hackeng, T. M., and Griffin, J. H. (1996) Binding sites for blood coagulation factor Xa and protein S involving residues 493-506 in factor Va, *Protein Science : a publication of the Protein Society 5*, 1883-1889.

[45] Kojima, Y., Heeb, M. J., Gale, A. J., Hackeng, T. M., and Griffin, J. H. (1998) Binding site for blood coagulation factor Xa involving residues 311-325 in factor Va, *Journal of Biological Chemistry 273*, 14900-14905.

[46] Lechtenberg, B. C., Murray-Rust, T. A., Johnson, D. J., Adams, T. E., Krishnaswamy, S., Camire, R. M., and Huntington, J. A. (2013) Crystal structure of the prothrombinase complex from the venom of Pseudonaja textilis, *Blood 122*, 2777-2783.

[47] Pomowski, A., Ustok, F. I., and Huntington, J. A. (2014) Homology model of human prothrombinase based on the crystal structure of Pseutarin C, *Biological Chemistry 395*, 1233-1241.

[48] Manithody, C., and Rezaie, A. R. (2005) Functional mapping of charged residues of the 82-116 sequence in factor Xa: evidence that lysine 96 is a factor Va independent recognition site for prothrombin in the prothrombinase complex, *Biochemistry 44*, 10063-10070.

[49] Shim, J. Y., Lee, C. J., Wu, S., and Pedersen, L. G. (2015) A model for the unique role of factor Va A2 domain extension in the human ternary thrombin-generating complex, *Biophysical Chemistry 199*, 46-50.

[50] Previtali, E., Bucciarelli, P., Passamonti, S. M., and Martinelli, I. (2011) Risk factors for venous and arterial thrombosis, *Blood Transfusion 9*, 120-138.

[51] Novotny, W. F., Brown, S. G., Miletich, J. P., Rader, D. J., and Broze, G. J., Jr. (1991) Plasma antigen levels of the lipoprotein-associated coagulation inhibitor in patient samples, *Blood 78*, 387-393.

[52] Girard, T. J., Warren, L. A., Novotny, W. F., Likert, K. M., Brown, S. G., Miletich, J. P., and Broze, G. J., Jr. (1989) Functional significance of the Kunitz-type inhibitory domains of lipoprotein-associated coagulation inhibitor, *Nature 338*, 518-520.

[53] Wood, J. P., Ellery, P. E., Maroney, S. A., and Mast, A. E. (2014) Biology of tissue factor pathway inhibitor, *Blood 123*, 2934-2943.

[54] Burgering, M. J., Orbons, L. P., van der Doelen, A., Mulders, J., Theunissen, H. J., Grootenhuis, P. D., Bode, W., Huber, R., and Stubbs, M. T. (1997) The second Kunitz domain of human tissue factor pathway inhibitor: cloning, structure determination and interaction with factor Xa, *Journal of Molecular Biology 269*, 395-407.

[55] Bajaj, M. S., Birktoft, J. J., Steer, S. A., and Bajaj, S. P. (2001) Structure and biology of tissue factor pathway inhibitor, *Thrombosis and Haemostasis 86*, 959-972.

[56] Petersen, L. C., Bjørn, S. E., Olsen, O. H., Nordfang, O., Norris, F., and Norris, K. (1996) Inhibitory properties of separate recombinant Kunitz-type-protease-inhibitor domains from tissue-factor-pathway inhibitor, *European Journal of Biochemistry 235*, 310-316.

[57] Wesselschmidt, R., Likert, K., Girard, T., Wun, T. C., and Broze, G. J., Jr. (1992) Tissue factor pathway inhibitor: the carboxy-terminus is required for optimal inhibition of factor Xa, *Blood 79*, 2004-2010.

[58] Broze, G. J., Jr., Girard, T. J., and Novotny, W. F. (1990) Regulation of coagulation by a multivalent Kunitz-type inhibitor, *Biochemistry 29*, 7539-7546.

[59] Lindhout, T., Franssen, J., and Willems, G. (1995) Kinetics of the inhibition of tissue factor-factor VIIa by tissue factor pathway inhibitor, *Thrombosis and Haemostasis 74*, 910-915.

[60] Peraramelli, S., Thomassen, S., Heinzmann, A., Rosing, J., Hackeng, T. M., Hartmann, R., Scheiflinger, F., and Dockal, M. (2013) Direct inhibition of factor VIIa by TFPI and TFPI constructs, *Journal of Thrombosis and Haemostasis : JTH 11*, 704-714.

[61] Huang, Z. F., Wun, T. C., and Broze, G. J., Jr. (1993) Kinetics of factor Xa inhibition by tissue factor pathway inhibitor, *Journal of Biological Chemistry 268*, 26950-26955.

[62] Ndonwi, M., and Broze, G., Jr. (2008) Protein S enhances the tissue factor pathway inhibitor inhibition of factor Xa but not its inhibition of factor VIIa-tissue factor, *Journal of Thrombosis and Haemostasis : JTH 6*, 1044-1046.

[63] Lindhout, T., Salemink, I., Valentin, S., and Willems, G. M. (1996) Tissue Factor Pathway Inhibitor: Regulation Of Its Inhibitory Activity By Phospholipid Surfaces, *Pathophysiology of Haemostasis and Thrombosis 26(suppl 4)*, 89-97.

[64] Olson, S. T., Richard, B., Izaguirre, G., Schedin-Weiss, S., and Gettins, P. G. (2010) Molecular mechanisms of antithrombin-heparin regulation of blood clotting proteinases. A paradigm for understanding proteinase regulation by serpin family protein proteinase inhibitors, *Biochimie 92*, 1587-1596.

[65] Huntington, J. A. (2005) Chapter 13 - Heparin Activation of Serpins, In *Chemistry and Biology of Heparin and Heparan Sulfate* (Garg, H. G., Linhardt, R. J., and Hales, C. A., Eds.), pp 367-398, Elsevier Science, Amsterdam.

[66] Johnson, D. J., Li, W., Adams, T. E., and Huntington, J. A. (2006) Antithrombin-S195A factor Xa-heparin structure reveals the allosteric mechanism of antithrombin activation, *The EMBO journal 25*, 2029-2037.

[67] Krishnaswamy, S., Field, K. A., Edgington, T. S., Morrissey, J. H., and Mann, K. G. (1992) Role of the membrane surface in the activation of human coagulation factor X, *Journal of Biological Chemistry 267*, 26110-26120.

[68] Krishnaswamy, S. (1990) Prothrombinase complex assembly. Contributions of protein-protein and protein-membrane interactions toward complex formation, *Journal of Biological Chemistry 265*, 3708-3718.

[69] Rosing, J., Tans, G., Govers-Riemslag, J. W., Zwaal, R. F., and Hemker, H. C. (1980) The role of phospholipids and factor Va in the prothrombinase complex, *Journal of Biological Chemistry 255*, 274-283.

[70] Gilbert, G. E., Furie, B. C., and Furie, B. (1990) Binding of human factor VIII to phospholipid vesicles, *Journal of Biological Chemistry 265*, 815-822.

[71] Furie, B., Bouchard, B. A., and Furie, B. C. (1999) Vitamin K-dependent biosynthesis of gamma-carboxyglutamic acid, *Blood 93*, 1798-1808.

[72] Mizuno, H., Fujimoto, Z., Atoda, H., and Morita, T. (2001) Crystal structure of an anticoagulant protein in complex with the Gla domain of factor X, *Proceedings of the National Academy of Sciences of the United States of America 98*, 7230-7234.

[73] Colpitts, T. L., Prorok, M., and Castellino, F. J. (1995) Binding of calcium to individual gamma-carboxyglutamic acid residues of human protein C, *Biochemistry 34*, 2424-2430.

[74] Persson, E., and Petersen, L. C. (1995) Structurally and functionally distinct Ca2+ binding sites in the gamma-carboxyglutamic acid-containing domain of factor VIIa, *European Journal of Biochemistry 234*, 293-300.

[75] Ratcliffe, J. V., Furie, B., and Furie, B. C. (1993) The importance of specific gamma-carboxyglutamic acid residues in prothrombin. Evaluation by site-specific mutagenesis, *Journal of Biological Chemistry 268*, 24339-24345.

[76] Christiansen, W. T., Jalbert, L. R., Robertson, R. M., Jhingan, A., Prorok, M., and Castellino, F. J. (1995) Hydrophobic amino acid residues of human anticoagulation protein C that contribute to its functional binding to phospholipid Vesicles, *Biochemistry 34*, 10376-10382.

[77] Huang, M., Rigby, A. C., Morelli, X., Grant, M. A., Huang, G., Furie, B., Seaton, B., and Furie, B. C. (2003) Structural basis of membrane binding by Gla domains of vitamin K-dependent proteins, *Nature Structural Biology 10*, 751-756.

[78] Ohkubo, Y. Z., and Tajkhorshid, E. (2008) Distinct structural and adhesive roles of Ca2+ in membrane binding of blood coagulation factors, *Structure (London, England : 1993) 16*, 72-81.

[79] Vadivel, K., Agah, S., Messer, A. S., Cascio, D., Bajaj, M. S., Krishnaswamy, S., Esmon, C. T., Padmanabhan, K., and Bajaj, S. P. (2013) Structural and functional studies of γ-carboxyglutamic acid domains of factor VIIa and activated Protein C: role of magnesium at physiological calcium, *Journal of Molecular Biology 425*, 1961-1981.

[80] Agah, S., and Bajaj, S. P. (2009) Role of magnesium in factor XIa catalyzed activation of factor IX: calcium binding to factor IX under physiologic magnesium, *Journal of Thrombosis and Haemostasis : JTH 7*, 1426-1428.

[81] Wang, S. X., Hur, E., Sousa, C. A., Brinen, L., Slivka, E. J., and Fletterick, R. J. (2003) The extended interactions and Gla domain of blood coagulation factor Xa, *Biochemistry 42*, 7959-7966.

[82] Shikamoto, Y., Morita, T., Fujimoto, Z., and Mizuno, H. (2003) Crystal structure of Mg2+- and Ca2+-bound Gla domain of factor IX complexed with binding protein, *Journal of Biological Chemistry 278*, 24090-24094.

[83] Persson, E., and Ostergaard, A. (2007) Mg(2+) binding to the Gla domain of factor X influences the interaction with tissue factor, *Journal of Thrombosis and Haemostasis : JTH 5*, 1977-1978.

[84] Prendergast, F. G., and Mann, K. G. (1977) Differentiation of metal ion-induced transitions of prothrombin fragment 1, *Journal of Biological Chemistry 252*, 840-850.

[85] Sekiya, F., Yoshida, M., Yamashita, T., and Morita, T. (1996) Magnesium(II) is a crucial constituent of the blood coagulation cascade. Potentiation of coagulant activities of factor IX by Mg2+ ions, *Journal of Biological Chemistry 271*, 8541-8544.

[86] McDonald, J. F., Shah, A. M., Schwalbe, R. A., Kisiel, W., Dahlbäck, B., and Nelsestuen, G. L. (1997) Comparison of naturally occurring vitamin K-dependent proteins: correlation of amino acid sequences and membrane binding properties suggests a membrane contact site, *Biochemistry 36*, 5120-5127.

[87] Häfner, A., Merola, F., Duportail, G., Hutterer, R., Schneider, F. W., and Hof, M. (2000) Calcium-induced conformational change in fragment 1-86 of factor X, *Biopolymers 57*, 226-234.

[88] Sunnerhagen, M., Olah, G. A., Stenflo, J., Forsén, S., Drakenberg, T., and Trewhella, J. (1996) The relative orientation of Gla and EGF domains in coagulation factor X is altered by Ca2+ binding to the first EGF domain. A combined NMR-small angle X-ray scattering study, *Biochemistry 35*, 11547-11559.

[89] Valcarce, C., Selander-Sunnerhagen, M., Tämlitz, A. M., Drakenberg, T., Björk, I., and Stenflo, J. (1993) Calcium affinity of the NH2-terminal epidermal growth factor-like module of factor X. Effect of the gamma-carboxyglutamic acid-containing module, *Journal of Biological Chemistry 268*, 26673-26678.

[90] Persson, E., Björk, I., and Stenflo, J. (1991) Protein structural requirements for Ca2+ binding to the light chain of factor X. Studies using isolated intact fragments containing the gamma-carboxyglutamic acid region and/or the epidermal growth factor-like domains, *Journal of Biological Chemistry 266*, 2444-2452.

[91] Sunnerhagen, M., Forsén, S., Hoffrén, A. M., Drakenberg, T., Teleman, O., and Stenflo, J. (1995) Structure of the Ca(2+)-free Gla domain sheds light on membrane binding of blood coagulation proteins, *Nature Structural Biology 2*, 504-509.

[92] Erb, E. M., Stenflo, J., and Drakenberg, T. (2002) Interaction of bovine coagulation factor X and its glutamic-acid-containing fragments with phospholipid membranes. A surface plasmon resonance study, *European Journal of Biochemistry 269*, 3041-3046.

[93] Mallik, S., Prasad, R., Bhattacharya, A., and Sen, P. (2018) Synthesis of Phosphatidylserine and Its Stereoisomers: Their Role in Activation of Blood Coagulation, *ACS Medicinal Chemistry Letters 9*, 434-439.

[94] Tavoosi, N., Davis-Harrison, R. L., Pogorelov, T. V., Ohkubo, Y. Z., Arcario, M. J., Clay, M. C., Rienstra, C. M., Tajkhorshid, E., and Morrissey, J. H. (2011) Molecular determinants of phospholipid synergy in blood clotting, *Journal of Biological Chemistry 286*, 23247-23253.

[95] Neuenschwander, P. F., Bianco-Fisher, E., Rezaie, A. R., and Morrissey, J. H. (1995) Phosphatidylethanolamine augments factor VIIa-tissue factor activity: enhancement of sensitivity to phosphatidylserine, *Biochemistry 34*, 13988-13993.

[96] Muller, M. P., Wang, Y., Morrissey, J. H., and Tajkhorshid, E. (2017) Lipid specificity of the membrane binding domain of coagulation factor X, *Journal of Thrombosis and Haemostasis : JTH 15*, 2005-2016.

[97] Skogen, W. F., Bushong, D. S., Johnson, A. E., and Cox, A. C. (1983) The role of the Gla domain in the activation of bovine coagulation factor X by the snake venom protein XCP, *Biochemical and Biophysical Research Communications 111*, 14-20.

[98] Tans, G., and Rosing, J. (2001) Snake venom activators of factor X: an overview, *Haemostasis 31*, 225-233.

[99] Takeda, S., Igarashi, T., and Mori, H. (2007) Crystal structure of RVV-X: an example of evolutionary gain of specificity by ADAM proteinases, *FEBS letters 581*, 5859-5864.

[100] Zwaal, R. F. A., Comfurius, P., and Bevers, E. M. (1998) Lipid-protein interactions in blood coagulation, *Biochim. Biophys. Acta 1376*, 433-453.

[101] Bevers, E. M., Comfurius, P., Dekkers, D. W., Harmsma, M., and Zwaal, R. F. (1998) Transmembrane phospholipid distribution in blood cells: Control mechanisms and pathophysiological significance, *Biol. Chem. 379*, 973-986.

[102] Neuenschwander, P. F., and Morrissey, J. H. (1994) Roles of the membrane-interactive regions of factor VIIa and tissue factor. The factor VIIa Gla domain is dispensable for binding to tissue factor but important for activation of factor X, *J. Biol. Chem. 269*, 8007-8013.

[103] Kung, C., Hayes, E., and Mann, K. G. (1994) A membrane-mediated catalytic event in prothrombin activation, *J. Biol. Chem. 269*, 25838-25848.

[104] O'Donnell, V. B., Murphy, R. C., and Watson, S. P. (2014) Platelet lipidomics: modern day perspective on lipid discovery and characterization in platelets, *Circulation Research 114*, 1185-1203.

[105] Bevers, E. M., Comfurius, P., and Zwaal, R. F. A. (1983) Changes in membrane phospholipid distribution during platelet activation, *Biochim. Biophys. Acta 736*, 57-66.

[106] Smirnov, M. D., and Esmon, C. T. (1994) Phosphatidylethanolamine incorporation into vesicles selectively enhances factor Va inactivation by activated protein C, *Journal of Biological Chemistry. 269*, 816-819.

[107] Smeets, E. F., Comfurius, P., Bevers, E. M., and Zwaal, R. F. (1996) Contribution of different phospholipid classes to the prothrombin converting capacity of sonicated lipid vesicles, *Thrombsis Research. 81*, 419-426.

[108] Gilbert, G. E., and Arena, A. A. (1995) Phosphatidylethanolamine induces high affinity binding sites for factor VIII on membranes containing phosphatidyl-L-serine, *Journal of Biological Chemistry 270*, 18500-18505.

[109] Shaw, A. W., Pureza, V. S., Sligar, S. G., and Morrissey, J. H. (2007) The local phospholipid environment modulates the activation of blood clotting, *Journal of Biological Chemistry 282*, 6556-6563.

[110] Tavoosi, N., Davis-Harrison, R. L., Pogorelov, T. V., Ohkubo, Y. Z., Arcario, M. J., Clay, M. C., Rienstra, C. M., Tajkhorshid, E., and Morrissey, J. H. (2011) Molecular determinants of phospholipid synergy in blood clotting, *Journal of Biological Chemistry 286*, 23247-23253.

[111] Ritchie, T. K., Grinkova, Y. V., Bayburt, T. H., Denisov, I. G., Zolnerciks, J. K., Atkins, W. M., and Sligar, S. G. (2009) Chapter 11 - Reconstitution of membrane proteins in phospholipid bilayer nanodiscs, *Methods Enzymology. 464*, 211-231.

[112] Bayburt, T. H., Grinkova, Y. V., and Sligar, S. G. (2002) Self-assembly of discoidal phospholipid bilayer nanoparticles with membrane scaffold proteins, *Nano Letters 2*, 835-856.

[113] Fiske, C. H., and Subbarow, Y. (1925) The colorimetric determination of phosphorus, *Journal of Biological Chemistry 66*, 375-400.

[114] Terrettaz, S., Stora, T., Duschl, C., and Vogel, H. (1993) Protein binding to supported lipid membranes: investigation of the cholera toxin-ganglioside interaction by simultaneous impedance spectroscopy and surface plasmon resonance, *Langmuir : the ACS Journal of Surfaces and Colloids 9*, 1361-1369.

[115] Heyse, S., Vogel, H., Sänger, M., and Sigrist, H. (1995) Covalent attachment of functionalized lipid bilayers to planar waveguides for measuring protein binding to biomimetic membranes, *Protein Science. 4*, 2532-2544.

[116] Tavoosi, N., Smith, S. A., Davis-Harrison, R. L., and Morrissey, J. H. (2013) Factor VII and protein C are phosphatidic acid-binding proteins, *Biochemistry 52*, 5545-5552.

[117] Medfisch, S. M., Muehl, E. M., Morrissey, J. H., and Bailey, R. C. (2020) Phosphatidylethanolamine-phosphatidylserine binding synergy of seven coagulation factors revealed using Nanodisc arrays on silicon photonic sensors, *Science Reports 10*, 17407.

[118] Muller, M. P., Wang, Y., Morrissey, J. H., and Tajkhorshid, E. (2017) Lipid specificity of the membrane binding domain of coagulation factor X, *J. Thromb. Haemost. 15*, 2005-2016.

[119] Ohkubo, Y. Z., Morrissey, J. H., and Tajkhorshid, E. (2010) Dynamical view of membrane binding and complex formation of human factor VIIa and tissue factor, *Journal of Thrombsis and Haemostasis 8*, 1044-1053.

[120] Tavoosi, N., and Morrissey, J. H. (2014) Influence of membrane composition on the enhancement of factor VIIa/tissue factor activity by magnesium ions, *Thrombosis and Haemostasis 111*, 770-772.

[121] Bajaj, S. P., Schmidt, A. E., Agah, S., Bajaj, M. S., and Padmanabhan, K. (2006) High resolution structures of p-aminobenzamidine- and benzamidine-VIIa/soluble tissue factor: unpredicted conformation of the 192-193 peptide bond and mapping of Ca2+, Mg2+, Na+, and Zn2+ sites in factor VIIa, *Journal of Biological Chemistry 281*, 24873-24888.

[122] Banner, D. W., D'Arcy, A., Chène, C., Winkler, F. K., Guha, A., Konigsberg, W. H., Nemerson, Y., and Kirchhofer, D. (1996) The crystal structure of the complex of blood coagulation factor VIIa with soluble tissue factor, *Nature 380*, 41-46.

[123] Stearns, D. J., Kurosawa, S., Sims, P. J., Esmon, N. L., and Esmon, C. T. (1988) The interaction of a Ca2+-dependent monoclonal antibody with the protein C activation peptide region. Evidence for obligatory Ca2+ binding to both antigen and antibody, *Journal of Biological Chemistry 263*, 826-832.

[124] Rezaie, A. R., Fiore, M. M., Neuenschwander, P. F., Esmon, C. T., and Morrissey, J. H. (1992) Expression and purification of a soluble tissue factor fusion protein with an epitope for an unusual calcium-dependent antibody, *Protein Expression and Purification 3*, 453-460.

[125] Waters, E. K., and Morrissey, J. H. (2006) Restoring full biological activity to the isolated ectodomain of an integral membrane protein, *Biochemistry 45*, 3769-3774.

[126] Smith, S. A., and Morrissey, J. H. (2004) Rapid and efficient incorporation of tissue factor into liposomes, *Journal of Thrombosis and Haemostasis : JTH 2*, 1155-1162.

[127] Bayburt, T. H., and Sligar, S. G. (2010) Membrane protein assembly into Nanodiscs, *FEBS letters 584*, 1721-1727.

[128] Shaw, A. W., Pureza, V. S., Sligar, S. G., and Morrissey, J. H. (2007) The local phospholipid environment modulates the activation of blood clotting, *Journal of Biological Chemistry 282*, 6556-6563.

[129] M. Iqbal, M. A. G., B. Spaugh, F. Tybor, W. G. Gunn, M. Hochberg, T. Baehr-Jones, R. C. Bailey, L. C. Gunn. (2010) Label-Free Biosensor Arrays Based on Silicon Ring Resonators and High-Speed Optical Scanning Instrumentation., *IEEE Journal of Selected Topics in Quantum Electronics 16*, 654-661.

[130] Washburn, A. L., Gomez, J., and Bailey, R. C. (2011) DNA-encoding to improve performance and allow parallel evaluation of the binding characteristics of multiple antibodies in a surface-bound immunoassay format, *Analytical Chemistry 83*, 3572-3580.

[131] Phillips, J. C., Braun, R., Wang, W., Gumbart, J., Tajkhorshid, E., Villa, E., Chipot, C., Skeel, R. D., Kale, L., and Schulten, K. (2005) Scalable molecular dynamics with NAMD, *Journal of Computational Chemistry 26*, 1781-1802.

[132] Best, R. B., Zhu, X., Shim, J., Lopes, P. E. M., Mittal, J., Feig, M., and MacKerell, A. D. (2012) Optimization of the Additive CHARMM All-Atom Protein Force Field Targeting Improved Sampling of the Backbone phi, psi and Side-Chain chi(1) and chi(2) Dihedral Angles, *Journal of Chemical Theory and Computation 8*, 3257-3273.

[133] Klauda, J. B., Venable, R. M., Freites, J. A., O'Connor, J. W., Tobias, D. J., Mondragon-Ramirez, C., Vorobyov, I., MacKerell, A. D., and Pastor, R. W. (2010) Update of the CHARMM

All-Atom Additive Force Field for Lipids: Validation on Six Lipid Types, *Journal of Physical Chemistry B 114*, 7830-7843.

[134] Essmann, U., Perera, L., Berkowitz, M. L., Darden, T., Lee, H., and Pedersen, L. G. (1995) A Smooth Particle Mesh Ewald Method, *J Chemical Physics 103*, 8577-8593.

[135] Hans, C. A. (1983) Rattle: A "velocity" version of the shake algorithm for molecular dynamics calculations, *Journal of Computational Physics 52*, 24-34.

[136] Jean-Paul, R., Giovanni, C., and Herman, J. C. B. (1977) Numerical integration of the cartesian equations of motion of a system with constraints: molecular dynamics of n-alkanes, *Journal of Computational Physics 23*, 327-341.

[137] Martyna, G. J., Tobias, D. J., and Klein, M. L. (1994) Constant pressure molecular dynamics algorithms, *The Journal of Chemical Physics 101*, 4177-4189.

[138] William, H., Andrew, D., and Klaus, S. (1996) VMD: Visual molecular dynamics, *Journal of Molecular Graphics 14*, 33-38.

[139] Paul D, and J.H., M. (2021) Stoichiometric analysis reveals a unique phosphatidylserine binding site in coagulation factor X, *Journal of Thrombosis and Haemostasis*.

[140] Watzke, H. H., Lechner, K., Roberts, H. R., Reddy, S. V., Welsch, D. J., Friedman, P., Mahr, G., Jagadeeswaran, P., Monroe, D. M., and High, K. A. (1990) Molecular defect (Gla+14----Lys) and its functional consequences in a hereditary factor X deficiency (factor X "Vorarlberg"), *Journal of Biological Chemistry 265*, 11982-11989.

[141] Kasturiratne, A., Wickremasinghe, A. R., de Silva, N., Gunawardena, N. K., Pathmeswaran, A., Premaratna, R., Savioli, L., Lalloo, D. G., and de Silva, H. J. (2008) The global burden of snakebite: a literature analysis and modelling based on regional estimates of envenoming and deaths, *PLoS Medicine 5*, e218.

[142] Senji Laxme, R. R., Khochare, S., Attarde, S., Suranse, V., Iyer, A., Casewell, N. R., Whitaker, R., Martin, G., and Sunagar, K. (2021) Biogeographic venom variation in Russell's viper (Daboia russelii) and the preclinical inefficacy of antivenom therapy in snakebite hotspots, *PLoS Neglected Tropical Diseases 15*, e0009247.

[143] Favaloro, E. J. (2019) The Russell viper venom time (RVVT) test for investigation of lupus anticoagulant (LA), *American Journal of Hematology 94*, 1290-1296.

[144] Marsh, N. A. (1998) Use of snake venom fractions in the coagulation laboratory, *Blood Coagulation & Fibrinolysis : an International Journal in Haemostasis and Thrombosis 9*, 395-404.

[145] Gowda, D. C., Jackson, C. M., Hensley, P., and Davidson, E. A. (1994) Factor X-activating glycoprotein of Russell's viper venom. Polypeptide composition and characterization of the carbohydrate moieties, *Journal of Biological Chemistry 269*, 10644-10650.

[146] Smith, S. A., Mutch, N. J., Baskar, D., Rohloff, P., Docampo, R., and Morrissey, J. H. (2006) Polyphosphate modulates blood coagulation and fibrinolysis, *Proceedings of the National Academy of Sciences of the United States of America 103*, 903-908.

[147] Butler, J. E., Pringnitz, D. J., Martens, C. L., and Crouch, N. (1980) Bovine-associated mucoprotein: I. Distribution among adult and fetal bovine tissues and body fluids, *Differentiation; Research in Biological Diversity 17*, 31-40.

[148] Hanayama, R., Tanaka, M., Miwa, K., Shinohara, A., Iwamatsu, A., and Nagata, S. (2002) Identification of a factor that links apoptotic cells to phagocytes, *Nature 417*, 182-187.

[149] Hanayama, R., Tanaka, M., Miyasaka, K., Aozasa, K., Koike, M., Uchiyama, Y., and Nagata, S. (2004) Autoimmune disease and impaired uptake of apoptotic cells in MFG-E8-deficient mice, *Science (New York, N.Y.) 304*, 1147-1150.

[150] Hanayama, R., and Nagata, S. (2005) Impaired involution of mammary glands in the absence of milk fat globule EGF factor 8, *Proceedings of the National Academy of Sciences of the United States of America 102*, 16886-16891.

[151] Shi, J., and Gilbert, G. E. (2003) Lactadherin inhibits enzyme complexes of blood coagulation by competing for phospholipid-binding sites, *Blood 101*, 2628-2636.

[152] Andersen, M. H., Graversen, H., Fedosov, S. N., Petersen, T. E., and Rasmussen, J. T. (2000) Functional analyses of two cellular binding domains of bovine lactadherin, *Biochemistry 39*, 6200-6206.

[153] Del Vecchio, K., and Stahelin, R. V. (2018) Investigation of the phosphatidylserine binding properties of the lipid biosensor, Lactadherin C2 (LactC2), in different membrane environments, *Journal of Bioenergetics and Biomembranes 50*, 1-10.

[154] Shao, C., Novakovic, V. A., Head, J. F., Seaton, B. A., and Gilbert, G. E. (2008) Crystal structure of lactadherin C2 domain at 1.7A resolution with mutational and computational analyses of its membrane-binding motif, *Journal of Biological Chemistry 283*, 7230-7241.

[155] Mucchiano, G., Cornwell, G. G., 3rd, and Westermark, P. (1992) Senile aortic amyloid. Evidence for two distinct forms of localized deposits, *The American Journal of Pathology 140*, 871-877.

[156] Häggqvist, B., Näslund, J., Sletten, K., Westermark, G. T., Mucchiano, G., Tjernberg, L. O., Nordstedt, C., Engström, U., and Westermark, P. (1999) Medin: an integral fragment of aortic smooth muscle cell-produced lactadherin forms the most common human amyloid, *Proceedings of the National Academy of Sciences of the United States of America 96*, 8669-8674.

[157] Peng, S., Larsson, A., Wassberg, E., Gerwins, P., Thelin, S., Fu, X., and Westermark, P. (2007) Role of aggregated medin in the pathogenesis of thoracic aortic aneurysm and dissection, *Laboratory Investigation; a Journal of Technical Methods and Pathology 87*, 1195-1205.

[158] Qi, C., Zhang, H., Liu, L., Yang, R., Kang, T., Hao, W., Jin, G., and Jiang, T. (2014) Analysis of interactions between SNARE proteins using imaging ellipsometer coupled with microfluidic array, *Scientific Reports 4*, 5341.

[159] De Lio A. M., P. D., Jain R., Morrissey J.H., Pogorelov T.V. (2020) Proteins and Ions Compete for Membrane Interaction: the case of Lactadherin, *bioRxiv*

[160] Camire, R. M. (2021) Blood coagulation factor X: molecular biology, inherited disease, and engineered therapeutics, *Journal of Thrombosis and Thrombolysis 52*, 383-390.